

1 **Title: Effector prediction and characterization in the oomycete pathogen**
2 ***Bremia lactucae* reveal host-recognized WY domain proteins that lack the**
3 **canonical RXLR motif**

4

5 **Short title:** Effector prediction and characterization in the oomycete pathogen
6 *Bremia lactucae*

7

8 Kelsey Wood^{1,2}, Munir Nur¹, Juliana Gil^{1,3}, Kyle Fletcher¹, Kim Lakeman⁴, Ayumi
9 Gothberg¹, Tina Khuu¹, Jennifer Kopetzky¹, Archana Pandya¹, Mathieu Pel⁴, and
10 Richard Michelmore^{1,5, *}

11 ¹The Genome Center, University of California, Davis, USA

12 ²Integrative Genetics & Genomics Graduate Group, University of California, Davis,
13 USA

14 ³Plant Pathology Graduate Group, University of California, Davis, USA

15 ⁴Enza Zaden, Enkhuizen, The Netherlands

16 ⁵Departments of Plant Sciences, Molecular & Cellular Biology, Medical Microbiology
17 & Immunology, University of California, Davis, USA.

18

19 * Corresponding author

20 E-mail: rwmichelmore@ucdavis.edu

21

22

23

24 **Abstract**

25 Pathogens infecting plants and animals use a diverse arsenal of effector proteins to
26 suppress the host immune system and promote infection. Identification of effectors
27 in pathogen genomes is foundational to understanding mechanisms of pathogenesis,
28 for monitoring field pathogen populations, and for breeding disease resistance. We
29 identified candidate effectors from the lettuce downy mildew pathogen, *Bremia*
30 *lactucae*, using comparative genomics and bioinformatics to search for the WY
31 domain. This conserved structural element is found in *Phytophthora* effectors and
32 some other oomycete pathogens; it has been implicated in the immune-suppressing
33 function of these effectors as well as their recognition by host resistance proteins. We
34 predicted 54 WY domain containing proteins in isolate SF5 of *B. lactucae* that have
35 substantial variation in both sequence and domain architecture. These candidate
36 effectors exhibit several characteristics of pathogen effectors, including an N-
37 terminal signal peptide, lineage specificity, and expression during infection.
38 Unexpectedly, only a minority of *B. lactucae* WY effectors contain the canonical N-
39 terminal RXLR motif, which is a conserved feature in the majority of cytoplasmic
40 effectors reported in *Phytophthora* spp. Functional analysis effectors containing WY
41 domains revealed eleven out of 21 that triggered necrosis, which is characteristic of
42 the immune response on wild accessions and domesticated lettuce lines containing
43 resistance genes. Only two of the eleven recognized effectors contained a canonical
44 RXLR motif, suggesting that there has been an evolutionary divergence in sequence
45 motifs between genera; this has major consequences for robust effector prediction in
46 oomycete pathogens.

47 **Author Summary**

48 There is a microscopic battle that takes place at the molecular level during infection
49 of plants and animals by pathogens. Some of the weapons that pathogens battle with
50 are known as “effectors,” which are secreted proteins that enter host cells to alter
51 physiology and suppress the immune system. Effectors can also be a liability for plant
52 pathogens because plants have evolved ways to recognize these effectors, triggering
53 a defense response leading to localized cell death, which prevents the spread of the
54 pathogen. Here we used computer models to predict effectors from the genome
55 of *Bremia lactucae*, the causal agent of lettuce downy mildew. Three effectors were
56 demonstrated to suppress the basal immune system of lettuce. Eleven effectors were
57 recognized by one or more resistant lines of lettuce. In addition to contributing to our
58 understanding of the mechanisms of pathogenesis, this study of effectors is useful
59 for breeding disease resistant lettuce, decreasing agricultural reliance on fungicides.

60

61 **Introduction**

62 The phylum Oomycota includes some of the most devastating pathogens of
63 both plants and animals [1]. Although oomycetes resemble fungi in their filamentous
64 growth and infection structures, they are more closely related to brown algae than to
65 fungi [2]. Notable oomycetes include the plant pathogens causing late blight of potato
66 (*Phytophthora infestans*) [3], sudden oak death (*Phytophthora ramorum*) [4], root rot
67 (*Phytophthora* [5] and *Pythium* spp. [6,7]), white blister rust of *Brassica* spp. (*Albugo*
68 spp.) [8], and downy mildews (e.g. *Bremia*, *Peronospora*, *Plasmopara* spp.) [9], as well
69 as several important animal pathogens infecting fish (*Saprolegnia* spp.), shellfish

70 (*Aphanomyces astaci*), and mammals, including humans (*Pythium insidiosum*) [1,10].
71 Many types of plant and animal pathogens, including the oomycetes, secrete proteins
72 known as effectors to promote virulence by manipulating the physiology of the host
73 cells and by suppressing the host immune system [11]. In plants, effectors are also
74 determinants of resistance or susceptibility through their direct or indirect
75 interactions with cognate nucleotide-binding leucine rich repeat proteins (NLRs)
76 encoded by resistance genes [12]. Effectors are secreted from the pathogen and may
77 act extracellularly or they may be translocated into the cytoplasm [11]. One class of
78 translocated effectors from plant pathogenic oomycetes of the class Peronosporales,
79 which includes *Phytophthora* and the downy mildews, are the RXLR effectors, so
80 called for their N-terminal motif usually consisting of arginine, followed by any amino
81 acid, then followed by leucine and arginine. RXLR effectors also contain an N-terminal
82 signal peptide, which designates them for extracellular transport by way of the
83 endoplasmic reticulum and Golgi apparatus [13]. The RXLR motif is often associated
84 with a downstream EER motif, both of which have been associated with secretion
85 and/or translocation of effectors into the plant cell [13,14]. For some RXLR effectors,
86 such as Avr3a, the RXLR motif has been shown to be cleaved just prior to the EER
87 sequence and therefore plays a role in secretion rather than uptake into the host cell
88 [15]. The RXLR motif is similar in sequence to the PEXEL motif (RXLX[EDQ]) of the
89 distantly related malaria pathogen (*Plasmodium falciparum*) [16] and the TEXEL
90 motif of *Toxoplasma gondii* (RRLXX) [17], both of which are required for proteolytic
91 modification in the endoplasmic reticulum and destine effector proteins for
92 specialized export out of the cell [18].

93 The downy mildews and the related *Phytophthora* species have different
94 lifestyles (obligate biotrophy vs. facultative hemibiotrophy) [19]; however, their
95 effectors share similar features. Many effectors in the Peronosporales have RXLR and
96 EER motifs; although several alternative sequences to RXLR have been found in
97 downy mildews, including RVRN (ATR5 from *Hyaloperonospora arabidopsidis*) [20],
98 QXLR (*Pseudoperonospora cubensis*) [21], GKLR (*Bremia lactucae*) [22,23], and RXLK
99 (*Plasmopara halstedii*) [24]. The C-terminal effector domains of RXLR effectors from
100 *Phytophthora* and downy mildews also share some common sequence motifs and
101 structural features, such as the 24 to 30 amino acid W, Y, and L motifs, which were
102 first identified bioinformatically [25]. Structural analysis on four different RXLR
103 effectors from *Phytophthora infestans* (Avr3a and PexRD2), *P. capsici* (Avr3a11), and
104 the downy mildew pathogen *H. arabidopsidis* (ATR1) revealed that the W and Y motifs
105 form an alpha-helical fold that may play a role in protein-protein interactions [26–
106 29]. This effector-associated fold, termed the WY domain after its conserved
107 tryptophan and tyrosine residues, is structurally highly conserved between effectors
108 from multiple Peronosporales species, despite sharing less than 20% sequence
109 similarity across the whole domain [26][30]. The WY domain appears to be specific
110 to the Peronosporales and was predicted to be present in nearly half of the RXLR
111 effectors of *P. infestans* and a fourth of the RXLR effectors in *H. arabidopsidis* [26].

112 Functional studies of WY domain containing proteins have indicated that
113 certain residues in the WY domain are essential for the immune suppressing
114 functions of *P. sojae* Avr1b [31], *P. infestans* Avr3a [32], and *P. infestans* PexRD2 [33].
115 Furthermore, mutation of two conserved leucines in the WY domain of PexRD2

116 disrupted interaction with its target, MAPKKKε, consistent with this domain being
117 important for protein-protein interactions [33]. WY domain containing proteins
118 appear to interact with a variety of host targets, with Avr3a from *P. infestans* targeting
119 the E3 ligase CMPG1 [32], *P. infestans* PexRD54 targeting potato autophagy-related
120 protein ATG8 [34], PsAvh240 from *P. sojae* targeting an aspartic protease [35], and
121 PSR2 from *P. sojae* and *P. infestans* suppressing host RNA silencing through
122 interactions with dsRNA-binding protein DRB4 [36–38]. Mutation analysis of the
123 regions encoding the seven individual WY domains of PSR2 demonstrated differential
124 contributions of each domain to virulence of *P. sojae*, suggesting that the WY domain
125 may act as a module during effector evolution [30]. In addition to its roles in immune
126 suppression, the WY domain has been shown to be important for immune recognition
127 of the effector by nucleotide binding-leucine rich repeat (NB-LRR) resistance proteins
128 [39].

129 Effector annotation in oomycete genomes has often relied on sequence
130 similarity to known effectors or on prediction of conserved motifs, such as the RXLR
131 motif, or in the case of Crinklers, the LXLFLAK motif [3]. Due to the short length and
132 degeneracy of the RXLR sequence, the motif occurs frequently by chance; therefore,
133 there is a high false positive rate (>50%) using string-based searches [25]. HMM-
134 based searches have much lower false positive rates, but the false negative rate may
135 be higher if the genome of interest has diverged significantly from the species used to
136 build the HMM. Downy mildews have a narrow host range and pathogenicity-related
137 proteins are likely to show high lineage-specificity due to co-evolution with their
138 hosts. There is already evidence that downy mildew effectors show divergence from

139 the canonical RXLR motif [20,23,24], thus complementary approaches for effector
140 prediction that utilize other conserved features, such as the WY domain, are
141 necessary to fully characterize the repertoire. In addition, due to the importance of
142 the WY domain in effector function [31–33], WY domain containing proteins may be
143 better candidates for effectors than those containing only the RXLR motif.

144 To identify a more complete repertoire of candidate effectors in the reference
145 genome of *B. lactucae* and to test whether the WY domain is informative for
146 predicting effectors in the Peronosporales, we searched for this domain using an
147 HMM built from sequences of the WY domain in three *Phytophthora* species [27]. This
148 revealed additional effector candidates that had not been found using an RXLR-based
149 search; similar results were also obtained for other downy mildews and well-studied
150 *Phytophthora* species. These predicted WY proteins from *B. lactucae* had other
151 signatures of oomycete effectors, such as presence of a secretion signal, N-terminal
152 intrinsic disorder, lineage specificity, and expression during infection. A subset of the
153 predicted WY effectors suppressed the host immune system, while others elicited
154 programmed cell death in specific genotypes of lettuce, indicative of recognition by
155 host resistance proteins. Therefore, searches for the WY domains are highly useful for
156 identification of downy mildew effectors lacking the RXLR motif, which was
157 previously considered canonical for effectors of the Peronosporales.

158

159 **Results**

160 Our HMM search initially identified 59 candidate WY effectors encoded by the
161 gene models predicted in the *B. lactucae* SF5 assembly [40]; however, three pairs of

162 genes appeared to be allelic based on sequence similarity and read depth, leaving a
163 total of 55 non-redundant genes encoding candidate effectors (Figure 1A;
164 Supplemental Table 1). Signal peptides were predicted for 43 of these 55 proteins, of
165 which two proteins had a predicted transmembrane helix outside of the signal
166 peptide (Figure 1A). Several predicted WY proteins seemed to be missing their start
167 codons due to N-terminal truncation when compared to close relatives. One of these
168 predicted proteins, BLN06, was found to be missing a significant portion of the N-
169 terminal sequence in SF5 compared to BL24, which was the source isolate for the
170 cloning of *BLN06* reported in Pelgrom *et al.* [41].

171 The N-terminal sequences of the 55 predicted WY effectors were examined for
172 the RXLR motif using both HMMs and string searches. One protein was predicted to
173 have an RXLR motif by the HMM and an additional 10 proteins were identified by a
174 string search for [RQGH]xLR or RXL[QKG], while 33 proteins were predicted to have
175 an EER motif using a string search for [DE][DE][EK] (Figure 1A). To find divergent
176 RXLR-like motifs in the WY effector candidates, we searched for a highly degenerate
177 pattern based on mutational studies of the RXLR motif [35] and natural RXLR variants
178 reported for other downy mildews [5–9]. This revealed an additional 38 proteins with
179 an RXLR-like motif within the first 60 amino acids after the signal peptide matching
180 the pattern [RKHGQ][X]{0,1}[LMYFIV][RNK], many of which also had an EER motif
181 (Figure 1A) (Supplemental Table 1). Therefore, the majority of candidate WY
182 effectors in *B. lactucae* have a non-canonical RXLR motif. In the C-terminal domain,
183 the WY effector candidates had one to seven WY domains per protein, with a diversity
184 of domain architectures (Figure 1). The WY domain from *B. lactucae* showed high

185 conservation of the characteristic conserved tryptophan (W) residue but appeared to
186 show equal preference for tyrosine (Y) or phenylalanine (F) for the second
187 characteristic residue of the domain (Fig. 1B). To investigate whether or not there are
188 WY effector candidates that are lacking the canonical RXLR motif in other oomycetes,
189 the predicted open reading frames (ORFs) from several published oomycete genomes
190 were surveyed for the RXLR motif and the WY domain. Approximately half of the WY
191 proteins predicted in seven downy mildew species lacked the RXLR motif; in six
192 *Phytophthora* spp., the majority of predicted WY proteins had RXLR motifs, but
193 between 9–21% of secreted WY proteins did not contain this motif (Fig. 2).
194 Consequently, the repertoire of candidate WY effectors in other oomycetes may be
195 heavily under-reported.

196 Intrinsic disorder had previously been reported to be a characteristic of the N-
197 terminus of oomycete effectors containing the RXLR motif [42]. Therefore, we
198 investigated whether the predicted degree of structural disorder was a characteristic
199 of candidate WY effectors lacking a canonical RXLR. The predicted levels of intrinsic
200 disorder were calculated for proteins containing RXLR motifs, for proteins containing
201 WY domains but no RXLR motif, as well as for the entire predicted secretome for
202 comparison. Proteins containing RXLR and/or WY domains had higher levels of
203 intrinsic disorder at their N-termini after the highly ordered signal peptide than the
204 entire set of secreted proteins (Fig. 3). Proteins containing a WY domain but lacking
205 a canonical RXLR motif had on average more disordered N-termini than effectors that
206 had RXLR but not a WY domain. The WY domain containing region had higher levels
207 of predicted structure than the RXLR-containing proteins that lacked a WY domain

208 and the secreted proteins as a whole (Fig. 3), consistent with the WY domains forming
209 an α -helix bundled structure [27]. This predicted pattern of high intrinsic disorder at
210 the N-terminus and high structure towards the C-terminus was consistently observed
211 in all six downy mildews and six *Phytophthora* species analyzed (Suppl. Fig. 2).
212 Therefore, a high level of intrinsic disorder is a consistent characteristic of the N-
213 termini of oomycete effectors, regardless of whether they have a canonical RXLR
214 motif; the functional significance of this remains to be investigated.

215 To evaluate lineage specificity of effectors due to co-evolution of pathogens
216 with their hosts, we used BLAST to identify orthologs in other oomycete species. All
217 of the 39 predicted secreted candidate WY effectors of *B. lactucae* had little sequence
218 similarity to sequences in other genomes with the best BLASTP hit being only 46%
219 identity with a protein from *P. infestans* (Fig. 4). Most of the proteins had best-hit
220 identities between 20 to 30%, which is similar to the level of amino acid conservation
221 between WY domains in different effectors [27].

222 A time-course RNA-seq experiment of lettuce seedlings infected with *B.*
223 *lactucae* isolate SF5 was analyzed to investigate the expression of the WY effector
224 candidates during infection. Expression was detected for all candidate WY encoding
225 genes. The four mostly highly expressed WY containing effectors lacked a canonical
226 RXLR motif (Fig. 5).

227 To test whether *B. lactucae* WY effectors were recognized by the host immune
228 system, 21 randomly-selected WY effectors that differed in their number of WY
229 domains were chosen to be screened against lettuce germplasm. Genes were cloned
230 from amplified genomic DNA to attempt to capture both alleles of each effector from

231 the heterozygous isolate SF5 [40]. In order to capture additional allelic diversity,
232 some effectors were also cloned from the heterokaryotic isolate C82P24 [40]. Two
233 alleles were obtained for many effectors; in addition, chimeric sequences appeared to
234 be obtained for several genes. Clones of all unique sequences for each effector were
235 retained because they could be informative for dissecting the sequence basis of host
236 recognition. This resulted in multiple distinct clones (wildtype alleles plus chimeric
237 sequences) of some effectors.

238 We screened 215 different accessions of wild and cultivated lettuce (Suppl.
239 File 2) using *Agrobacterium*-mediated transient expression for the elicitation of cell
240 death for their reactions to clones representing the 21 WY candidate effectors. These
241 accessions collectively express the majority of the known *Dm* genes as well as new
242 resistance factors [36]. Eleven of the 21 WY effectors were recognized by one or more
243 accessions (Fig. 6). Alleles of the same effector showed similar reactions except for
244 three genes (Fig. 6). The truncated version of BLN06 cloned from SF5 did not trigger
245 cell death in LS102, NunDm17, or RYZ2146 (Suppl. Figure 3) in contrast to BLN06
246 cloned from BL24 [41], suggesting that the recognition of this effector by these
247 genotypes may be determined by the N-terminal region of the effector after the
248 secretion signal.

249 The lines ViAE and ViCQ, which have introgressions from the wild lettuce
250 species *L. virosa* [43], recognized five effectors: BLN08, BSW03, BSW04m, BSW04p,
251 and BSW14, as well as the chimeric sequence BSW04m/p (Fig. 6A). The *L. virosa*
252 accessions that were the resistance donors for ViAE and ViCQ also recognized these
253 five effectors, but not the chimeric sequence BSW04m/p (Fig. 6B). Many *L. sativa*

254 cultivars and a few genotypes of *L. saligna* and *L. serriola* were observed to have
255 necrosis or yellowing in response to the chimeric effector BSW04m/p, suggestive of
256 a non-specific reaction to this unnatural protein. Some of the genotypes that
257 recognized BSW04m/p also recognized BSW04p, but not the paralog BSW04m. Three
258 of these genotypes, Capitan, Ninja, and Femke, share the resistance gene *Dm11*;
259 therefore, we tested two additional cultivars, Fila and Mondian, which also contain
260 *Dm11* for recognition of BSW04p. These varieties also recognized BSW04m/p and
261 BSW04p, but not BSW04m. Due to recognition of BSW04p by multiple varieties that
262 contain *Dm11*, BSW04p is a candidate for the protein encoded by the *Avr11* gene.
263 BLN08, BSW03, BSW04m, and BSW14 are candidate avirulence proteins for which
264 cognate *Dm* genes have yet to be identified.

265 Bioinformatic prediction of subcellular localization using NucPred [44]
266 suggested that BSW04p had a C-terminal nuclear localization signal (score 0.79). To
267 investigate whether BSW04p was nuclear localized, N-terminal yellow fluorescent
268 protein (YFP) fusions were expressed in lettuce using *Agrobacterium*-mediated
269 transient assays. We also made N-terminal YFP fusions of two other effectors, BLN08
270 and BSW03, which lacked predicted nuclear localization signals. BSW04p was
271 localized to the nucleus as predicted, while BLN08 and BSW03 were localized to the
272 cytoplasm and/or periplasm (Fig. 7). Therefore, predictions of subcellular
273 localization were accurate for these three effectors and may indicate the cellular
274 location of their targets during infection.

275 We also tested candidate effectors for their ability to suppress PAMP-triggered
276 immunity (PTI). Twenty-one effectors were transiently expressed in *Nicotiana*

277 *benthamiana* and the level of reactive oxygen species (ROS) production induced by
278 flg22 was measured. Three effectors significantly suppressed ROS production to a
279 similar extent as two known bacterial suppressors of PTI (Fig. 8). The level of
280 induction of ROS by flg22 was significantly higher with some effectors; however,
281 there was no induction of ROS in the absence of flg22. Therefore, in this assay, at least
282 three effectors suppress PTI and some may actually increase PTI responsiveness.

283

284 **Discussion**

285 Effectors play a critical role in interactions between pathogens and their hosts.
286 Accurate prediction and annotation of effector repertoires is foundational for
287 functional genomics studies of pathogens. Due to their economic importance in
288 agriculture, an increasing number of *Phytophthora* and downy mildew pathogens are
289 being sequenced. Prior to this study, the majority of cloned avirulence genes have
290 encoded proteins with a RXLR motif [45]. This was not surprising considering that
291 most of these studies used the RXLR motif as their primary, or only, criterion to
292 identify candidate effectors. Our results demonstrate that there are many candidate
293 effectors containing the effector-related WY domain that lack the canonical RXLR
294 motif, especially in the downy mildews, but also in *Phytophthora* spp. In *B. lactucae*,
295 we have shown that these non-RXLR, WY domain containing effectors show
296 characteristics of RXLR effectors, such as N-terminal intrinsic disorder, lineage
297 specificity, and expression during infection. Furthermore, some of these proteins can
298 act as suppressors of the host immune system, while others trigger the hypersensitive
299 response in resistant host cultivars. Thus, despite lacking the canonical RXLR-motif,

300 these WY domain containing proteins have both virulence and avirulence activity.
301 Consequently, numerous candidate effector genes are likely to have been missed in
302 the genomic analysis of other species within the Peronosporales. Bioinformatics
303 pipelines for predicting effectors in both *Phytophthora* spp. and downy mildew
304 pathogens should include an HMM for the WY domain because it may be more
305 informative of function and result in fewer false positives than string searches for the
306 RXLR motif.

307 Many WY effectors were initially predicted to not have a signal peptide and
308 therefore not to be secreted; this could have been due to misannotation or reflect
309 biological reality. Several had a predicted signal peptide downstream of the ATG in
310 the gene model; these signal peptides started with a methionine, which was
311 supported as the correct start in manual curation using RNAseq data. Therefore,
312 studies that rely on the presence of a signal peptide when using predicted ORFs may
313 be missing true effectors with misannotated start codons. Some WY effectors had
314 clearly lost the signal peptide due to N-terminal deletion; this was observed by
315 comparisons within effector families. The truncated effectors are unlikely to be
316 functional because they are missing the secretion signal and would not therefore be
317 secreted from the cell. Signal peptide loss may be an evolutionary strategy for the
318 pathogen to evade recognition of effectors.

319 Although very few of the WY effectors from *B. lactucae* contained the canonical
320 RXLR motif, nearly all of them contained a degenerate RXLR motif. However, the
321 degenerate RXLR regular expression should not be used on its own to search for genes
322 encoding RXLR proteins due to the high false positive rate (>50%). Functional studies

323 are needed to ascertain which of these degenerate motifs can function similarly to the
324 canonical RXLR motif in protein secretion [15]. Despite lacking the canonical RXLR
325 motif, the WY effectors had other features similar to RXLR proteins such as high N-
326 terminal intrinsic disorder and the presence an EER motif. N-terminal intrinsic
327 disorder has been predicted for RXLR effectors of *Phytophthora* and is also a common
328 feature of bacterial effectors [46]. The biological significance of these features
329 remains to be studied, particularly whether these intrinsically disordered domains
330 are important in post-translational modification or protein-protein interactions as is
331 the case for intrinsically disordered regions in other organisms [47,48].

332 The number of WY domains per protein varied considerably, from one to
333 seven in *B. lactucae*. Many pathogen effectors exhibit rapid evolution and divergence
334 due to selective pressure of evolving host targets and host resistance proteins [25].
335 Duplication of domains may allow for evolution of novel effector functions or for
336 evasion of host recognition while retaining function [30]. Variation in the number of
337 repeated domains is reminiscent of NB-LRR proteins, which recognize effectors
338 (and/or effector activity) and also have leucine-rich repeated domains [49,50].
339 Duplication of regions encoding WY domains may have happened within a gene
340 through replication errors or between different genes through illegitimate
341 recombination. The genomic sequences of the repeats will be analyzed in multiple
342 isolates to reveal the origins of these duplications and domain expansion or
343 contraction.

344 Analysis of the amino acid sequences of the WY domain in *B. lactucae* showed
345 that it may be better considered as a W[Y/F] domain, due to the equal preference for

346 phenylalanine and tyrosine for the second characteristic residue. This substitution
347 has a BLOSUM score of 3, indicating that it is fairly common. Both tyrosine and
348 phenylalanine are aromatic amino acids; however, the hydroxyl group on tyrosine
349 makes it slightly bulkier, more polar, and introduces a potential phosphorylation site.
350 Variation in this region is not uncommon in other oomycete species: the fifth of the
351 seven domains in Psr2 of *P. sojae* has an F instead of a Y and is similar in structure to
352 the single domain of ATR1 in *H. arabidopsidis* that has a cysteine at the Y position [30].
353 Further structural characterization is needed to reveal whether these substitutions
354 alter protein structure and their biological function.

355 In oomycetes, WY domain containing effectors have been shown to have
356 several functions including PTI suppression [51]. At least three WY effectors from *B.*
357 *lactucae* were able to suppress the host immune system by interfering with pathogen-
358 triggered production of ROS. Suppression of host defenses is critical to the survival of
359 *B. lactucae* and therefore it is not surprising that multiple effectors target the basal
360 immune system. Identification of the host targets of these effectors will determine
361 which steps in the signal transduction cascade are modulated by each effector or may
362 reveal candidates for susceptibility genes in the host that are required for successful
363 proliferation of *B. lactucae*.

364 Effectors are powerful tools for the discovery and characterization of host
365 resistance genes [52]. Eleven of the *B. lactucae* effectors tested were recognized by
366 one or more lettuce lines. Their cognate R genes will be identified using mapping of
367 segregating F_{2:3} and recombinant inbred line populations. Recognition of four *B.*
368 *lactucae* effectors (BLG01, BLN08, BLR31, and BLR38) has been successfully mapped

369 [23,41,53]. BLG01 and BLN08 have been shown to be recognized broadly by *L. saligna*
370 [23,53]. Our study confirms the results for BLN08 and revealed BSW14 as an
371 additional effector recognized by *L. saligna*. BLN08 and BSW14 share little sequence
372 similarity (besides containing WY domains). Non-host resistance in *L. saligna* is
373 clearly complex [54], but these results show that it is mediated in part by recognition
374 of multiple effectors.

375 Not all RXLR candidate effectors have WY domains and the presence of a WY
376 domain is not required for the avirulence activity of all effectors; for example, the *B.*
377 *lactucae* effectors BLG01 and BLG03 do not contain WY domains, yet they elicit an
378 immune response in lettuce [23]. Structural elucidation of an RXLR effector lacking
379 the WY motif, *H. arabidopsidis* ATR13, revealed that it contained a helical fold that
380 was distinct from the WY fold [55]. It would be informative to determine and compare
381 the protein structures of additional RXLR effectors to determine whether there are
382 other conserved C-terminal domains that may be involved in effector function in a
383 similar way as the WY domain.

384 Both RXLR and WY effectors provide tools for monitoring pathogen
385 populations and effector-driven resistance breeding. Analysis of diverse, global
386 isolates will allow the characterization of individual effector repertoires as well as the
387 development of the pan-repertoire for a whole pathogen species. Effectors also will
388 be highly instrumental in cloning their cognate resistance genes as well as the
389 identification of effector targets in the host. In addition, screens for resistance using
390 transient expression of individual effectors will allow the pyramiding of resistance
391 genes with different specificities that will maximize the evolutionary hurdle for the

392 pathogen to become virulent. Ultimately, knowledge of effector repertoires will allow
393 data-driven deployment of resistance genes leading to more durable disease
394 resistance [56].

395

396 **Materials and Methods**

397

398 *Effector prediction*

399 To search for the WY domain, a Hidden Markov Model (HMM) was built using
400 HMMer v3.1 [57] based on the inferred amino acid sequences of WY domains from *P.*
401 *infestans*, *P. sojae*, and *P. ramorum*. These sequences were obtained from the
402 supplemental material of Boutemy *et al.* [27] who predicted genes encoding WY
403 domains based on motif searches of candidate RXLR effectors and identified a 49
404 amino acid long motif that spanned the WY domain in the crystal structures of
405 Avr3a11 and PexRD2 [26]. Candidate WY effectors were predicted using this HMM to
406 search translated predicted ORF sequences (>80 amino acids) as well as gene models
407 in the draft genome of *B. lactucae* isolate SF5 [40]. Sequences with a positive HMM bit
408 score were considered to be putative WY domain effectors as in [27]. Signal peptide
409 prediction was performed on candidate WY effectors using SignalP v 4.1 [58] and
410 PhobiusSP [59]. Default settings were altered for SignalP v 4.1 to have sensitivity
411 similar to SignalP v 3.0. Output was compared between SignalP v 4.1 sensitive and the
412 combination of SignalP4.0 + SignalP 3.0, and identical results were obtained from the
413 two methods. Gene models were more accurate for predicting signal peptides than
414 translated ORFs — in part due to misannotated start codons upstream of the probable

415 true start codon and signal peptides in the ORFs. However, on several occasions the
416 gene model was missing a signal peptide found in the ORF – these gene models were
417 manually updated to reflect this likely true start site. SignalP v 4.1 in sensitive mode
418 was better able to predict signal peptides in proteins with misannotated start codons
419 compared to SignalP v 4.0 or v 5.0.

420

421 *RXLR prediction*

422 A combination of string searches and HMMs were used to search for the RXLR motif
423 in oomycete predicted WY proteins. The following strings were used based on
424 variants observed in downy mildews: [RQGH]xLR or RXL[QKG] for RXLR and
425 [DE][DE][KR] for EER. The Whisson *et al.* HMM [14] was also tested, although this did
426 not reveal any more RXLR effector candidates. To search for additional non-canonical
427 RXLR motifs in WY candidates, a highly degenerate string of
428 [RKHGQ][X]{0,1}[LMYFIV][RNK] was used.

429

430 *Estimation of false positive rates for effector prediction*

431 We determined false positive rates for each motif by analyzing multiple permutations
432 of the non-redundant secretome using the same pipeline as described above for
433 effector prediction. At least ten random permutations of the sequence space were
434 created using the MEME fasta-shuffle-letters program (with a kmer size of 1) using
435 peptides starting after the cleavage site identified by SignalP v4.1. The false positive
436 rate for each motif was estimated as the average frequency of detection in the
437 permuted sequences divided by the observed frequency in the original sequences.

438 The estimated false positive rate for the RXLR and WY motif searches are given in
 439 Table 1.

440

441 **Table 1. False positive rates for RXLR and WY HMM and string searches across**
 442 **14 oomycete genomes**

Motif	String/HMM	False Positive Rate (Average +SD)	Range
RXLR	RXLR	45.2% ± 3.4%	32-54%
RXLR	[RQGH]XLR or RXL[QKG]	56% ± 2%	50-64%
RXLR	Whisson HMM [14]	1.5% ± 0.8%	0.1-3.3%
EER	[DE][DE][KR]	49.4% ± 2.6%	41-62%
RXLR-EER	RXLR + [DE][DE][KR]	9.4% ± 3.0%	4-16%
Degenerate RXLR	[RKHGQ][X]{0,1}[LMYFIV][RNK]	74% ± 0.8%	71-77%
WY	Boutemy HMM [27]	0.05% ± 0.09%	0-0.3%

443

444 *Intrinsic Disorder*

445 PONDRL VSL2 [60] was used to calculate levels of intrinsic disorder for groups
 446 of candidate effectors, grouped by the presence of an RXLR-like motif, EER-like motif,
 447 and/or WY domain. PONDRL VSL2 is a meta-predictor of protein disorder that utilizes
 448 neural networks and amino acid context to give a weighted disorder score at each
 449 amino acid position. The average sequence disorder was calculated at each amino
 450 acid position in each group of effectors and aligned on the first amino acid. Plots were
 451 generated from the average positional disorder scores calculated from all peptides in
 452 a group. The entire non-redundant, predicted secretome was used as a reference for
 453 comparison.

454

455 *Sequence comparison and determination of lineage specificity*

456 To generate a neighbor-joining tree of the WY effector candidates, whole
457 protein amino acid alignments were performed using MUSCLE 3.8.425 [61]
458 implemented in Geneious 11.0.5 (<http://www.geneious.com>) with default settings. A
459 UPGMA tree was built in Geneious with bootstrap resampling (100 replicates). The
460 resulting tree was annotated using the Interactive Tree of Life [62] and stylistically
461 refined in the GNU Image Manipulation Program (<http://www.gimp.org>). To build a
462 sequence logo for the WY domain from *B. lactucae*, a multiple sequence alignment of
463 WY domains was built using MUSCLE 3.8.425 [61], was manually corrected for
464 alignment errors, and the sequence logo generated using Weblogo
465 (<http://weblogo.berkeley.edu/logo.cgi>).

466 To determine if the candidate WY proteins are unique to *B. lactucae*, BLASTp
467 [63] was used to search for orthologs in other oomycete species. BLASTp-based
468 sequence comparisons with an e-value threshold of 0.01 were performed against the
469 following oomycete genomes: *Albugo laibachii* [8], *H. arabidopsidis* [64], *P. capsici*
470 [65], *P. infestans* [3], *Phytophthora parasitica* [66], *P. ramorum* [5], *P. sojae* [5],
471 *Pythium ultimum* [7], *Saprolegnia parasitica* [67], *Pseudoperonospora cubensis* [21],
472 *Plasmopara halstedii* [24], *Plasmopara viticola* JL-7-2 [68], INRA-PV221 [69],
473 *Peronospora tabacina* [70], and *Peronospora effusa* [71].

474

475 *RNA-seq analysis*

476 Messenger RNA was isolated from cotyledons of lettuce cv. Cobham Green
477 infected with isolate SF5 of *B. lactucae* with Dynabeads™ mRNA DIRECT™

478 Purification kit (Thermo Fisher Scientific, Waltham, MA) per manufacturer
479 recommendations for plant tissue. Library construction was done following the
480 protocol of Zhong *et al.* [72]. The resulting libraries were sequenced in single-end
481 mode in a HiSeq 3000 at the UC Davis DNA Technologies Core
482 (<http://dnatech.genomecenter.ucdavis.edu/>). The quality of the libraries was
483 assessed using FastQC V0.11.2 [73]. Bacterial and human contaminants were filtered
484 with BWA-MEM [74] mapping against custom references of microbial and human
485 databases. The remaining reads were mapped to a joint reference made up of the *L.*
486 *sativa* cv. Salinas (GenBank: GCF_002870075.1) and *B. lactucae* isolate SF5 (GenBank:
487 GCA_004359215.1) reference assemblies using STAR v2.6.0 [75]. STAR was run with
488 the options “--sjdbOverhang 99 --sjdbGTFtagExonParentGene Parent --quantMode
489 GeneCounts”. The strand specific read counts for each replicate were calculated from
490 the reads per gene table output by STAR. Reads counts were normalized for gene
491 length by dividing the read counts by the length of the gene it was mapped to (Reads
492 Per Kilobase: RPK). The total RPK of the *B. lactucae* portion of each replicate was
493 calculated and used to divide the RPK to calculate the transcripts per million (TPM)
494 for each gene. A subset of the genes that encode putative WY domains were taken
495 from this total, the average TPM for three replicates of each time point was calculated
496 (excluding replicate 2 at 72 hours, due to low coverage) and the $\log_{10}(1+\text{average}$
497 $\text{TPM})$ was calculated for each time point. These values were plotted using Heatmap2
498 [76] from the package gplots, clustering of putative effectors by expression was
499 performed with hclust [77].

500

501 *Gateway cloning*

502 Effector candidates without their signal peptide were cloned into the
503 pEarleyGate100 (pEG100) vector for plant expression [78] using Gateway cloning
504 (Thermo Fisher Scientific). Candidate effector genes were amplified from genomic
505 DNA isolated from spores of *B. lactucae* isolate SF5 or C82P24 using Phusion High
506 Fidelity Polymerase (Thermo Fisher Scientific) and primers (Suppl. File 3) that
507 amplified each ORF after the predicted signal peptide cleavage site. The Kozak
508 sequence (ACCATG) was added to the forward primer for correct translational
509 initiation. PCR products were purified using polyethylene glycol (PEG) precipitation
510 to remove primers and primer-dimers, recombined into pDONR207 using BP Clonase
511 II (Thermo Fisher Scientific), and transformed into chemically competent *Escherichia*
512 *coli* DH10B cells. The resulting entry clones were sequenced using primers designed
513 to pDONR207 to confirm gene identity and identify alleles. The entry clones were
514 then recombined into pEG100 using LR Clonase II and transformed into *E. coli* to
515 generate expression clones. The expression clones were then transformed into
516 *Agrobacterium tumefaciens* strain C58rif⁺ using electroporation. Kanamycin-resistant
517 colonies were confirmed for the transgene using gene-specific primers.

518

519 *Agrobacterium-mediated transient assays*

520 Agroinfiltration and transient expression experiments were performed using
521 conditions optimized for lettuce [79]. *A. tumefaciens* was grown overnight from
522 glycerol stocks and resuspended in 10 mM MgCl₂ to OD=0.3–0.5. The youngest fully
523 expanded leaves of 3 to 4-week-old greenhouse grown lettuce plants were infiltrated

524 with the *A. tumefaciens* cultures using a needleless syringe. Leaves were examined four
525 to five days post-infiltration for signs of macroscopic cell death, indicative of immune
526 recognition by host resistance proteins. *A. tumefaciens* containing pEG100 empty
527 vector or pEG100:GFP were used as negative controls; *A. tumefaciens* containing T-
528 DNAs that expressed HopM1 or AvrPto, which are *Pseudomonas syringae* effectors
529 known to elicit cell death in lettuce [80], were used as positive controls. To control
530 for false negatives, leaves that did not show cell death in response to the positive
531 control HopM1 were excluded from the analysis. To control for false positives, leaves
532 that showed cell death in response to the empty vector or GFP control were also
533 excluded from the analysis. In addition, any cell death observed in the initial
534 screening was confirmed by repeating infiltrations on at least four plants for effectors
535 found to cause cell death.

536

537 *Subcellular localization prediction and characterization*

538 Nuclear localization was predicted using NucPred [44] and nuclear
539 localization motifs predicted using LOCALIZER [81]. For localization experiments,
540 effectors were cloned without their signal peptide into pEG104 [31] as described
541 above resulting in an N-terminal YFP fusion. Three to five days post-Agroinfiltration,
542 lettuce leaves expressing N-terminal YFP fusions of effectors were examined for
543 subcellular localization. Nuclear staining was performed by incubating cut leaf tissue
544 in 18 nM DAPI in water for at least five minutes. Imaging was performed on a Zeiss
545 LSM 710 laser scanning confocal microscope with a 40x objective lens.

546

547 *PTI suppression assay*

548 Effectors were expressed in five-week-old plants of *N. benthamiana* using
549 Agrobacterium infiltration as described above. Two days post-infiltration, two leaf discs (3.8
550 mm) were taken from each infiltration site away from the leaf veins using a cork
551 borer. Leaf discs were floated abaxial side up in 200 μ L of distilled water in a 96-well
552 white assay plate and incubated at room temperature for 24 hrs. To measure
553 suppression of ROS production [82], the water was removed and 100 μ L of assay
554 solution was added to the leaf discs, which contained 17 μ g/mL luminol (Sigma-
555 Aldrich, St Louis, MO) and 10 μ g/mL horseradish peroxidase type 6A (Sigma-Aldrich).
556 One of the two paired leaf discs was exposed to 100 nM of flg22 peptide (flg+) and the
557 other was not exposed to any elicitor as a control for endogenous ROS production.
558 The known bacterial suppressors of PTI, HopS2, and HopX1 [83], were used as
559 positive controls for suppression of ROS production; GFP was used as the negative
560 control. Luminescence was measured on a FilterMax F5 Plate Reader (Molecular
561 Devices, San Jose, CA) promptly after adding in the assay solution and was measured
562 every two minutes for a total of 42 minutes. Each assay was replicated sixteen times.

563

564 **Acknowledgements**

565 We thank Keri Cavanaugh, Alyssa Schweickert, Dasan Gann, Catherine Lopez, Amber
566 Robbins, Natalie Hamada, Pauline Sanders, and Sebastian Reyes Chin Wo (all UC
567 Davis) for wet lab and computational assistance. We thank Gitta Coaker (UC Davis)
568 for assistance with the ROS assay. We thank Brigitte Maisonneuve (INRA, Montfavet,
569 France) for providing the FrRsal-1, ViAE, and ViCQ lines of lettuce and Ales Lebeda

570 (Palacký University, Olomouc, Czech Republic) and Alex Beharav (The Hebrew
571 University, Tel Aviv, Israel) for lines of *L. saligna*. We thank Lien Bertier, Dasan Gann,
572 Anne Giesbers, and Elizabeth Georgian for helpful comments on earlier versions of
573 this manuscript. The work was supported by an NSF Graduate Fellowship and a USDA
574 Fellowship #2018-67011-28053 to KW and the NSF/USDA AFRI Microbial
575 Sequencing Program award #2009-65109-05925 to RWM.

576

577 **Author Contributions**

578 KW, JG, MP, and RWM conceived and designed the experiments. KW, JG, TK, MN, AP,
579 AG, JK, and KL performed the experiments. KW, JG, KF, TK, MN, AP, AG, JK, and KL
580 analyzed the data. KW, JG, and RWM wrote the paper. All authors approved the final
581 submission.

582

583 **Data sources**

584 The reference genome assembly of *B. lactucae* is available from NCBI, GenBank ID:
585 GCA_004359215.1. RNAseq reads of lettuce cv. Cobham Green infected with *B.*
586 *lactucae* isolate SF5 is available at NCBI SRA BioProject PRJNA523226. Sequences of
587 effector proteins are available in Supplementary data. The all data for interactions
588 between effectors and individual lines of *Lactuca* spp. are available at
589 http://bremia.ucdavis.edu/BIL/BIL_interaction.php.

590

591 **References**

592 1. Derevnina L, Petre B, Kellner R, Dagdas YF, Sarowar MN, Giannakopoulou A, et

- 593 al. Emerging oomycete threats to plants and animals. *Philos Trans R Soc B Biol*
594 *Sci.* 2016;371. doi:10.1098/rstb.2015.0459
- 595 2. Baldauf SL. The Deep Roots of Eukaryotes. 2003;300: 1703–1707.
596 doi:10.1126/science.1085544
- 597 3. Haas BJ, Kamoun S, Zody MC, Jiang RHY, Handsaker RE, Cano LM, et al.
598 Genome sequence and analysis of the Irish potato famine pathogen
599 *Phytophthora infestans*. *Nature.* 2009;461: 393–398.
600 doi:10.1038/nature08358
- 601 4. Rizzo DM, Garbelotto M, Hansen EM. *Phytophthora ramorum*: Integrative
602 Research and Management of an Emerging Pathogen in California and Oregon
603 Forests. *Annu Rev Phytopathol.* 2005;43: 309–335.
604 doi:10.1146/annurev.phyto.42.040803.140418
- 605 5. Tyler BM, Tripathy S, Zhang X, Dehal P, Jiang RHY, Aerts A, et al. *Phytophthora*
606 genome sequences uncover evolutionary origins and mechanisms of
607 pathogenesis. *Science.* 2006;313: 1261–1266. doi:10.1126/science.1128796
- 608 6. Adhikari BN, Hamilton JP, Zerillo MM, Tisserat N, Lévesque CA, Buell CR.
609 Comparative genomics reveals insight into virulence strategies of plant
610 pathogenic oomycetes. *PLoS One.* 2013;8: e75072.
611 doi:10.1371/journal.pone.0075072
- 612 7. Lévesque CA, Brouwer H, Cano L, Hamilton JP, Holt C, Huitema E, et al.
613 Genome sequence of the necrotrophic plant pathogen *Pythium ultimum*
614 reveals original pathogenicity mechanisms and effector repertoire. *Genome*

- 615 Biol. 2010;11: 1–22. doi:10.1186/gb-2010-11-7-r73
- 616 8. Kemen E, Gardiner A, Schultz-Larsen T, Kemen AC, Balmuth AL, Robert-
617 Seilaniantz A, et al. Gene gain and loss during evolution of obligate parasitism
618 in the white rust pathogen of *Arabidopsis thaliana*. PLoS Biol. 2011;9:
619 e1001094. doi:10.1371/journal.pbio.1001094
- 620 9. Thines M, Choi Y. Evolution, Diversity, and Taxonomy of the Peronosporaceae,
621 with Focus on the Genus *Peronospora*. Phytopathology. 2015;106: 6–18.
- 622 10. Phillips AJ, Anderson VL, Robertson EJ, Secombes CJ, van West P. New insights
623 into animal pathogenic oomycetes. Trends Microbiol. 2007;16: 13–19.
624 doi:10.1016/j.tim.2007.10.013
- 625 11. Bozkurt TO, Schornack S, Banfield MJ, Kamoun S. Oomycetes, effectors, and all
626 that jazz. Curr Opin Plant Biol. Elsevier Ltd; 2012;15: 483–92.
627 doi:10.1016/j.pbi.2012.03.008
- 628 12. Jones JDG, Dangl JL. The plant immune system. Nature. 2006;444: 323–329.
629 doi:10.1038/nature05286
- 630 13. Birch PRJ, Armstrong M, Bos J, Boevink P, Gilroy EM, Taylor RM, et al. Towards
631 understanding the virulence functions of RXLR effectors of the oomycete plant
632 pathogen *Phytophthora infestans*. J Exp Bot. 2009;60: 1133–1140.
633 doi:10.1093/jxb/ern353
- 634 14. Whisson SC, Boevink PC, Moleleki L, Avrova AO, Morales JG, Gilroy EM, et al. A
635 translocation signal for delivery of oomycete effector proteins into host plant
636 cells. Nature. 2007;450: 115–118. doi:10.1038/nature06203

- 637 15. Wawra S, Trusch F, Matena A, Apostolakis K, Linne U, Zhukov I, et al. The
638 RxLR Motif of the Host Targeting Effector AVR3a of *Phytophthora infestans* Is
639 Cleaved Before Secretion. *Plant Cell*. 2017;29: tpc.00552.2016.
640 doi:10.1105/tpc.16.00552
- 641 16. Hiller NL, Hiller NL, Bhattacharjee S, Ooij C Van, Liolios K, Harrison T, et al. A
642 Host-Targeting Signal in Virulence Proteins Reveals a Secretome in Malarial
643 Infection. *Science* (80-). 2012;1934: 1934–1938.
644 doi:10.1126/science.1102737
- 645 17. Coffey MJ, Sleebis BE, Uboldi AD, Garnham A, Franco M, Marino ND, et al. An
646 aspartyl protease defines a novel pathway for export of *Toxoplasma* proteins
647 into the host cell. *Elife*. 2015;4: 1–34. doi:10.7554/eLife.10809
- 648 18. Boddey JA, O’Neill MT, Lopaticki S, Carvalho TG, Hodder AN, Nebl T, et al.
649 Export of malaria proteins requires co-translational processing of the PEXEL
650 motif independent of phosphatidylinositol-3-phosphate binding. *Nat*
651 *Commun*. 2016;7. doi:10.1038/ncomms10470
- 652 19. Thines M. Bridging the gulf: *Phytophthora* and downy mildews are connected
653 by rare grass parasites. Ausubel FM, editor. *PLoS One*. Public Library of
654 *Science*; 2009;4: e4790. doi:10.1371/journal.pone.0004790
- 655 20. Bailey K, Cevik V, Holton N, Byrne-Richardson J, Sohn KH, Coates M, et al.
656 Molecular cloning of ATR5(Emoy2) from *Hyaloperonospora arabidopsidis*, an
657 avirulence determinant that triggers RPP5-mediated defense in *Arabidopsis*.
658 *Mol Plant Microbe Interact*. 2011;24: 827–838. doi:10.1094/MPMI-12-10-

- 659 0278
- 660 21. Tian M, Win J, Savory E, Burkhardt A, Held M, Brandizzi F, et al. 454 Genome
661 sequencing of *Pseudoperonospora cubensis* reveals effector proteins with a
662 QXLR translocation motif. *Mol Plant Microbe Interact. The American*
663 *Phytopathological Society*; 2011;24: 543–53. doi:10.1094/MPMI-08-10-0185
- 664 22. Stassen J, Seidl M. Effector identification in the lettuce downy mildew *Bremia*
665 *lactucae* by massively parallel transcriptome sequencing. *Mol Plant Pathol.*
666 2012;13: 719–31. doi:10.1111/j.1364-3703.2011.00780.x
- 667 23. Stassen JHM, Boer E den, Vergeer PWJ, Andel A, Ellendorff U, Pelgrom K, et al.
668 Specific In Planta Recognition of Two GCLR Proteins of the Downy Mildew
669 *Bremia lactucae* Revealed in a Large Effector Screen in Lettuce. *Mol Plant*
670 *Microbe Interact. The American Phytopathological Society*; 2013;26: 1259–
671 1270. doi:10.1094/MPMI-05-13-0142-R
- 672 24. Sharma R, Xia X, Cano LM, Evangelisti E, Kemen E, Judelson H, et al. Genome
673 analyses of the sunflower pathogen *Plasmopara halstedii* provide insights into
674 effector evolution in downy mildews and *Phytophthora*. *BMC Genomics. BMC*
675 *Genomics*; 2015;16: 741. doi:10.1186/s12864-015-1904-7
- 676 25. Jiang RHY, Tripathy S, Govers F, Tyler BM. RXLR effector reservoir in two
677 *Phytophthora* species is dominated by a single rapidly evolving superfamily
678 with more than 700 members. *Proc Natl Acad Sci U S A.* 2008;105: 4874–
679 4879. doi:10.1073/pnas.0709303105
- 680 26. Win J, Krasileva K V, Kamoun S, Shirasu K, Staskawicz BJ, Banfield MJ.

- 681 Sequence divergent RXLR effectors share a structural fold conserved across
682 plant pathogenic oomycete species. PLoS Pathog. 2012;8: e1002400.
683 doi:10.1371/journal.ppat.1002400
- 684 27. Boutemy L, King S, Win J, Hughes R, Clarke T, Blumenschein T, et al. Structures
685 of Phytophthora RXLR effector proteins a conserved but adaptable fold
686 underpins functional diversity. J Biol Chem. 2011;286: 35834–42.
687 doi:10.1074/jbc.M111.262303
- 688 28. Chou S, Krasileva K V, Holton JM, Steinbrenner AD, Alber T, Staskawicz BJ.
689 Hyaloperonospora arabidopsidis ATR1 effector is a repeat protein with
690 distributed recognition surfaces. Proc Natl Acad Sci U S A. 2011;108: 13323–
691 13328. doi:10.1073/pnas.1109791108
- 692 29. Yaeno T, Li H, Chaparro-Garcia A, Schornack S, Koshiba S, Watanabe S, et al.
693 Phosphatidylinositol monophosphate-binding interface in the oomycete RXLR
694 effector AVR3a is required for its stability in host cells to modulate plant
695 immunity. Proc Natl Acad Sci. National Academy of Sciences; 2011;108:
696 14682–14687. doi:10.1073/PNAS.1106002108
- 697 30. He J, Ye W, Choi DS, Wu B, Zhai Y, Guo B, et al. Structural analysis of
698 *Phytophthora* suppressor of RNA silencing 2 (PSR2) reveals a conserved
699 modular fold contributing to virulence. Proc Natl Acad Sci. 2019;2:
700 201819481. doi:10.1073/pnas.1819481116
- 701 31. Dou D, Kale SD, Wang X, Chen Y, Wang Q, Wang X, et al. Conserved C-terminal
702 motifs required for avirulence and suppression of cell death by *Phytophthora*

- 703 sojae effector Avr1b. *Plant Cell*. 2008;20: 1118–1133.
704 doi:10.1105/tpc.107.057067
- 705 32. Bos JIB, Armstrong MR, Gilroy EM, Boevink PC, Hein I, Taylor RM, et al.
706 Phytophthora infestans effector AVR3a is essential for virulence and
707 manipulates plant immunity by stabilizing host E3 ligase CMPG1. *Proc Natl*
708 Acad Sci U S A. National Academy of Sciences; 2010;107: 9909–14.
709 doi:10.1073/pnas.0914408107
- 710 33. King SRF, McLellan H, Boevink PC, Armstrong MR, Bukharova T, Sukarta O, et
711 al. Phytophthora infestans RXLR Effector PexRD2 Interacts with Host
712 MAPKKK{varepsilon} to Suppress Plant Immune Signaling. *Plant Cell*.
713 2014;26: 1345–59. doi:10.1105/tpc.113.120055
- 714 34. Maqbool A, Hughes RK, Dagdas YF, Tregidgo N, Zess E, Belhaj K, et al.
715 Structural basis of host Autophagy-related protein 8 (ATG8) binding by the
716 Irish potato famine pathogen effector protein PexRD54. *J Biol Chem*. 2016;8:
717 jbc.M116.744995. doi:10.1074/jbc.M116.744995
- 718 35. Guo B, Wang H, Yang B, Jiang W, Jing M, Li H, et al. Phytophthora sojae effector
719 PsAvh240 inhibits a host aspartic protease secretion to promote infection.
720 *Mol Plant*. Chinese Society for Plant Biology; 2019;
721 doi:10.1016/j.molp.2019.01.017
- 722 36. Qiao Y, Liu L, Xiong Q, Flores C, Wong J, Shi J, et al. Oomycete pathogens
723 encode RNA silencing suppressors. *Nat Genet*. Nature Publishing Group;
724 2013;45: 330–3. doi:10.1038/ng.2525

- 725 37. Xiong Q, Ye W, Choi D, Wong J, Qiao Y, Tao K, et al. Phytophthora Suppressor
726 of RNA Silencing 2 Is a Conserved RxLR Effector that Promotes Infection in
727 Soybean and Arabidopsis thaliana. Mol Plant- 2014;27: 1379–1389.
728 Available: [http://apsjournals.apsnet.org/doi/abs/10.1094/MPMI-06-14-](http://apsjournals.apsnet.org/doi/abs/10.1094/MPMI-06-14-0190-R)
729 0190-R
- 730 38. Hou Y, Zhai Y, Feng L, Karimi HZ, Rutter BD, Zeng L, et al. A Phytophthora
731 Effector Suppresses Trans-Kingdom RNAi to Promote Disease Susceptibility.
732 Cell Host Microbe. Elsevier Inc.; 2019;25: 153–165.e5.
733 doi:10.1016/j.chom.2018.11.007
- 734 39. Goritschnig S, Steinbrenner AD, Grunwald DJ, Staskawicz BJ. Structurally
735 distinct Arabidopsis thaliana NLR immune receptors recognize tandem WY
736 domains of an oomycete effector. New Phytol. 2016;210: 984–96.
- 737 40. Fletcher K, Gil J, Bertier LD, Kenefick A, Wood KJ, Zhang L, et al. Genomic
738 signatures of heterokaryosis in the oomycete pathogen Bremia lactucae. Nat
739 Commun. 2019;10: 2645. doi:10.1101/516526
- 740 41. Pelgrom AJE, Eikelhof J, Elberse J, Meisrimler CN, Raedts R, Klein J, et al.
741 Recognition of lettuce downy mildew effector BLR38 in Lactuca serriola
742 LS102 requires two unlinked loci. Molecular Plant Pathology. 2018: 240–253.
743 doi:10.1111/mpp.12751
- 744 42. Shen D, Li Q, Sun P, Zhang M, Dou D. Intrinsic disorder is a common structural
745 characteristic of RxLR effectors in oomycete pathogens. Fungal Biol. Elsevier
746 Ltd; 2017;121: 911–919. doi:10.1016/j.funbio.2017.07.005

- 747 43. Maisonneuve B. *Lactuca virosa*, a source of disease resistance genes for
748 lettuce breeding: results and difficulties for gene introgression. *Eucarpia leafy*
749 *Veg '03*. 2003;2003: 61–67. Available:
750 http://www.leafyvegetables.nl/download/12_061-067_maisonneuve.pdf
- 751 44. Brameier M, Krings A, MacCallum RM. NucPred - Predicting nuclear
752 localization of proteins. *Bioinformatics*. 2007;23: 1159–1160.
753 doi:10.1093/bioinformatics/btm066
- 754 45. Anderson RG, Deb D, Fedkenheuer K, Mcdowell JM. Recent Progress in RXLR
755 Effector Research. *Mol Plant Microbe Interact*. 2015;28: 1063–1072.
756 doi:10.1094/MPMI-01-15-0022-CR
- 757 46. Marin M, Uversky VN, Ott T. Intrinsic Disorder in Pathogen Effectors: Protein
758 Flexibility as an Evolutionary Hallmark in a Molecular Arms Race. *Plant Cell*.
759 2013;25: 3153–3157. doi:10.1105/tpc.113.116319
- 760 47. Uversky VN. Intrinsic disorder-based protein interactions and their
761 modulators. *Curr Pharm Des*. 2013;19: 4191–213. Available:
762 <http://www.ncbi.nlm.nih.gov/pubmed/23170892>
- 763 48. Iakoucheva LM, Brown CJ, Lawson JD, Obradović Z, Dunker AK. Intrinsic
764 Disorder in Cell-signaling and Cancer-associated Proteins. *J Mol Biol*.
765 2002;323: 573–584. doi:10.1016/S0022-2836(02)00969-5
- 766 49. Meyers BC, Kozik A, Griego A, Kuang H, Michelmore RW. Genome-Wide
767 Analysis of NBS-LRR – Encoding Genes in *Arabidopsis*. 2003;15: 809–834.
768 doi:10.1105/tpc.009308.During

- 769 50. Hofberger JA, Jones JDG. A Novel Approach for Multi-Domain and Multi-Gene
770 Family Identification Provides Insights into Evolutionary Dynamics of Disease
771 Resistance Genes in Core Eudicot Plants Netherlands Chinese Academy of
772 Sciences / Max Planck Partner Institute for Computational. 2014;31: 1–35.
- 773 51. He Q, McLellan H, Hughes RK, Boevink PC, Armstrong M, Lu Y, et al.
774 *Phytophthora infestans* effector SFI 3 targets potato UBK to suppress early
775 immune transcriptional responses. New Phytol. John Wiley & Sons, Ltd
776 (10.1111); 2018; np.15635. doi:10.1111/nph.15635
- 777 52. Vleeshouwers VGAA, Oliver RP. Effectors as tools in disease resistance
778 breeding against biotrophic, hemibiotrophic, and necrotrophic plant
779 pathogens. Mol Plant Microbe Interact. 2014;27: 196–206.
780 doi:10.1094/MPMI-10-13-0313-IA
- 781 53. Giesbers AKJ, Pelgrom AJE, Visser RGF, Niks RE, Van den Ackerveken G,
782 Jeuken MJW. Effector-mediated discovery of a novel resistance gene against
783 *Bremia lactucae* in a nonhost lettuce species. New Phytol. 2017;
784 doi:10.1111/nph.14741
- 785 54. Giesbers AKJ, Boer E Den, Braspenning DNJ, Bouten TPH, Specken JW, van
786 Kaauwen MPW, et al. Bidirectional backcrosses between wild and cultivated
787 lettuce identify loci involved in nonhost resistance to downy mildew. Theor
788 Appl Genet. Springer Berlin Heidelberg; 2018; 1–16. doi:10.1007/s00122-
789 018-3112-8
- 790 55. Leonelli L, Pelton J, Schoeffler A, Dahlbeck D, Berger J, Wemmer DE, et al.

- 791 Structural elucidation and functional characterization of the
792 *Hyaloperonospora arabidopsidis* effector protein ATR13. Tyler B, editor. PLoS
793 Pathog. Public Library of Science; 2011;7: e1002428.
794 doi:10.1371/journal.ppat.1002428
- 795 56. Michelmore RW, Christopoulou M, Caldwell KS. Impacts of resistance gene
796 genetics, function, and evolution on a durable future. Annu Rev Phytopathol.
797 2013;51: 291–319. doi:10.1146/annurev-phyto-082712-102334
- 798 57. Eddy SR. Accelerated Profile HMM Searches. PLoS Computational Biology.
799 2011. p. e1002195. doi:10.1371/journal.pcbi.1002195
- 800 58. Petersen TN, Brunak S, von Heijne G, Nielsen H. SignalP 4.0: discriminating
801 signal peptides from transmembrane regions. Nat Methods. Nature Publishing
802 Group; 2011;8: 785–786. doi:10.1038/nmeth.1701
- 803 59. Käll L, Krogh A, Sonnhammer ELL. Advantages of combined transmembrane
804 topology and signal peptide prediction-the Phobius web server. Nucleic Acids
805 Res. 2007;35: 429–432. doi:10.1093/nar/gkm256
- 806 60. Peng K, Radivojac P, Vucetic S, Dunker AK, Obradovic Z. Length-dependent
807 prediction of protein in intrinsic disorder. BMC Bioinformatics. 2006;7: 1–17.
808 doi:10.1186/1471-2105-7-208
- 809 61. Edgar RC. MUSCLE: multiple sequence alignment with high accuracy and high
810 throughput. Nucleic Acids Res. 2004;32: 1792–7. doi:10.1093/nar/gkh340
- 811 62. Letunic I, Bork P. Interactive Tree Of Life (iTOL): an online tool for
812 phylogenetic tree display and annotation. Bioinformatics. 2007;23: 127–8.

- 813 doi:10.1093/bioinformatics/btl529
- 814 63. Altschul SF, Gish W, Miller W, Myers EW, Lipman DJ. Basic local alignment
815 search tool. *J Mol Biol.* 1990;215: 403–410. doi:10.1016/S0022-
816 2836(05)80360-2
- 817 64. Baxter L, Tripathy S, Ishaque N, Boot N, Cabral A, Kemen E, et al. Signatures of
818 adaptation to obligate biotrophy in the *Hyaloperonospora arabidopsidis*
819 genome. *Science* (80-). 2010;330: 1549–1551. doi:10.1126/science.1195203
- 820 65. Lamour KH, Mudge J, Gobena D, Hurtado-Gonzales OP, Schmutz J, Kuo A, et al.
821 Genome sequencing and mapping reveal loss of heterozygosity as a
822 mechanism for rapid adaptation in the vegetable pathogen *Phytophthora*
823 *capsici*. [Internet]. *Molecular plant-microbe interactions : MPMI.* 2012. pp.
824 1350–60. doi:10.1094/MPMI-02-12-0028-R
- 825 66. Broad Institute. *Phytophthora parasitica* INRA-310 Genome sequencing and
826 assembly. [Internet]. 2018 [cited 6 Jun 2018]. Available:
827 [https://data.nal.usda.gov/dataset/phytophthora-parasitica-inra-310-](https://data.nal.usda.gov/dataset/phytophthora-parasitica-inra-310-genome-sequencing-and-assembly)
828 genome-sequencing-and-assembly
- 829 67. Jiang RHY, de Bruijn I, Haas BJ, Belmonte R, Löbach L, Christie J, et al.
830 Distinctive Expansion of Potential Virulence Genes in the Genome of the
831 Oomycete Fish Pathogen *Saprolegnia parasitica*. *PLoS Genet.* 2013;9:
832 e1003272. doi:10.1371/journal.pgen.1003272
- 833 68. Yin L, An Y, Qu J, Li X, Zhang Y, Dry I, et al. Genome sequence of *Plasmopara*
834 *viticola* and insight into the pathogenic mechanism. *Sci Rep.* Nature

- 835 Publishing Group; 2017;7: 1–12. doi:10.1038/srep46553
- 836 69. Dussert Y, Couture C, Mazet ID, Gouzy J, Piron M-C, Kuchly C, et al. Genome
837 assembly and annotation of *Plasmopara viticola*, the grapevine downy mildew
838 pathogen [Internet]. Portail Data Inra; 2019. doi:doi/10.15454/4NYHD6
- 839 70. Derevnina L, Reyes-Chin Wo S, Martin F, Wood K, Froenicke L, Spring O, et al.
840 Genome Sequence and Architecture of the Tobacco Downy Mildew Pathogen,
841 *Peronospora tabacina*. *Mol plant-microbe Interact*. 2015;28: 1198–1215.
842 doi:10.1094/MPMI-05-15-0112-R
- 843 71. Fletcher K, Klosterman SJ, Derevnina L, Martin F, Bertier LD, Koike S, et al.
844 Comparative genomics of downy mildews reveals potential adaptations to
845 biotrophy. *BMC Genomics*. *BMC Genomics*; 2018;19: 8–10.
846 doi:10.1186/s12864-018-5214-8
- 847 72. Zhong S, Joung JG, Zheng Y, Chen YR, Liu B, Shao Y, et al. High-throughput
848 illumina strand-specific RNA sequencing library preparation. *Cold Spring*
849 *Harb Protoc*. 2011;6: 940–949. doi:10.1101/pdb.prot5652
- 850 73. Andrews S. FastQC: a quality control tool for high throughput sequence data
851 [Internet]. 2010.
- 852 74. Li H. Aligning sequence reads, clone sequences and assembly contigs with
853 BWA-MEM. 2013;00: 1–3. doi:10.1186/s13756-018-0352-y
- 854 75. Dobin A, Davis CA, Schlesinger F, Drenkow J, Zaleski C, Jha S, et al. STAR:
855 Ultrafast universal RNA-seq aligner. *Bioinformatics*. 2013;29: 15–21.
856 doi:10.1093/bioinformatics/bts635

- 857 76. Warnes GR, Bolker B, Bonebakker L, Gentleman R, Huber W, Liaw A, et al.
858 Package 'gplots' [Internet]. 2012. Available: <http://cran.r-project.org>
- 859 77. Team RC. R: A language and environment for statistical computing. [Internet].
860 Vienna, Austria.: R Foundation for Statistical Computing; 2014. Available:
861 <http://www.r-project.org/>
- 862 78. Earley KW, Haag JR, Pontes O, Opper K, Juehne T, Song K, et al. Gateway-
863 compatible vectors for plant functional genomics and proteomics. *Plant J.*
864 2006;45: 616–629. doi:10.1111/j.1365-313X.2005.02617.x
- 865 79. Wroblewski T, Tomczak A, Michelmore R. Optimization of Agrobacterium-
866 mediated transient assays of gene expression in lettuce, tomato and
867 Arabidopsis. *Plant Biotechnol J.* 2005;3: 259–273. Available:
868 <http://www.ncbi.nlm.nih.gov/pubmed/17173625>
- 869 80. Wroblewski T, Caldwell KS, Piskurewicz U, Cavanaugh KA, Xu H, Kozik A, et al.
870 Comparative large-scale analysis of interactions between several crop species
871 and the effector repertoires from multiple pathovars of *Pseudomonas* and
872 *Ralstonia*. *Plant Physiol.* 2009;150: 1733–49. doi:10.1104/pp.109.140251
- 873 81. Sperschneider J, Catanzariti AM, Deboer K, Petre B, Gardiner DM, Singh KB, et
874 al. LOCALIZER: Subcellular localization prediction of both plant and effector
875 proteins in the plant cell. *Sci Rep. Nature Publishing Group;* 2017;7: 1–14.
876 doi:10.1038/srep44598
- 877 82. Felix G, Duran JD, Volko S, Boller T. Plants have a sensitive perception system
878 for the most conserved domain of bacterial flagellin. *Plant J.* 1999;18: 265–

879 276. doi:10.1046/j.1365-313X.1999.00265.x

880 83. Jamir Y, Guo M, Oh HS, Petnicki-Ocwieja T, Chen S, Tang X, et al. Identification
881 of *Pseudomonas syringae* type III effectors that can suppress programmed
882 cell death in plants and yeast. *Plant J.* 2004;37: 554–565. doi:10.1046/j.1365-
883 313X.2003.01982.x

884

885

886

887

888

889 **Figure legends**

890

891 **Figure 1. WY effector candidates from *B. lactucae* isolate SF5.** (A) UPGMA
892 consensus tree of the 59 predicted WY effectors from *B. lactucae* isolate SF5 based
893 on whole protein amino acid sequence alignment using MUSCLE. Sequences that
894 appear to be allelic are indicated with asterisks next to the sequence name.
895 Bootstrap values and branch lengths are given for closely related proteins. Signal
896 peptides are shown as circles (red circle for SP; white circle for no SP). RXLR motifs
897 are shown as triangles (black triangle for RXLR ([RQGH]xLR or RXL[QKG]); grey
898 triangle for degenerate RXLR ([RKHGQ][X]{0,1}[LMYFIV][RNK]), white triangle for
899 no RXLR-like sequence) followed by an inverted triangle for EER motifs (yellow
900 triangle for [DE][DE][RK], white triangle for no EER-like sequence). WY domain
901 architecture is shown using blue rectangles, with a black line representing the total
902 length of the protein and rectangle position representing the location of the WY
903 motif as predicted by HMMer 3.0. (B) Sequence logo for the WY domain from *B.*
904 *lactucae* built from a multiple sequence alignment of WY domains predicted by
905 HMMer 3.0.

906

907 **Figure 2. Distribution of predicted secreted WY effectors with or without RXLR**
908 **and/or EER motifs in the genomes of downy mildew pathogens and**
909 ***Phytophthora* species.** HMMer was used to search predicted secretomes for each
910 species for the WY domain. For the WY domaining containing proteins, the presence

911 of RXLR and EER were determined by searching for [RQGH]XLR or RXL[QKG] within
912 the first 60 amino acids after the signal peptide and [DE][DE][KR] within the first
913 100 amino acids after the signal peptide. For the non-WY domain containing
914 proteins, the RXLR and EER was determined by searching for a strict “RXLR” with
915 [DE][DE][KR], within the first 60 and 100 amino acids, respectively, plus proteins
916 found by searching for the RXLR-EER domain using the RXLR-EER HMM from [14].

917

918 **Figure 3. Intrinsic disorder in the first 150 N-terminal amino acid sequences**
919 **of RXLR and/or WY containing candidate effectors in *B. lactuca*.** Proteins were
920 categorized as WY with no RXLR (yellow), WYs with RXLR (black), RXLR+EER (with
921 or without WY, purple), and the total predicted secretome (blue). RXLR and EER
922 motifs were as described in Fig 2. Average positional disorder scores [42] with
923 standard error are shown for each group of proteins.

924

925 **Figure 4. Lineage specificity of *B. lactuca* candidate secreted WY effectors.**
926 Secreted WY proteins predicted in isolate SF5 of *B. lactuca* were used as a query for
927 BLASTp against other oomycete translated ORFs. Isolate C82P24 was queried for *B.*
928 *lactuca*. The best BLAST hit percent identity for each protein was calculated. The
929 box plot shows the distribution of the best BLAST hits per *B. lactuca* WY protein
930 from each species, with each dot representing an individual data point. No hits were
931 observed to *Albugo laibachii*, *Saprolegnia parasitica*, or *Pythium ultimum*.

932

933 **Figure 5. RNA-seq expression levels during infection for the *B. lactucae* WY**
934 **effector candidates.** The transcripts per million (TPM) of each WY-encoding gene
935 was normalized by the total number of reads per kilobase assigned to *B. lactucae*
936 from RNAseq analysis of infected cotyledons over a seven-day time-course. This
937 value was log₁₀(+1) transformed to enable visualization. The four highest
938 expressed WY encoding genes do not have recognizable RxLR translocation
939 associated motifs.

940

941 **Figure 6. Results of the screen for recognition of *B. lactucae* WY effector by**
942 **diverse genotypes of lettuce.** Candidate effectors were expressed in lettuce leaves
943 using Agroinfiltration and leaves were scored for their reaction four to seven days
944 post-infiltration. Qualitative scores were converted into numeric scores for data
945 analysis: 0 = no reaction (green), 1 = mild chlorosis (blue-green), 2 = chlorosis
946 (yellow), 3 = mild necrosis or mixture of chlorosis and necrosis (pink), and 4 = full
947 necrosis (magenta). The figure shows average scores for each effector on each
948 genotype; only accessions and effectors that had a necrotic or chlorotic response are
949 shown. Scores for all accessions screened and sample sizes can be found at
950 http://bremia.ucdavis.edu/BIL/BIL_interaction.php. Two groups of 28 and 11
951 accessions of *L. saligna* that had identical reactions are shown together; the
952 individual accessions making up each group are shown in Supplementary Table 2.

953

954 **Figure 7. Example Agroinfiltration results of reactions of *L. sativa* ViAE and**

955 **ViCQ and their progenitor R gene donors *L. virosa* LS238 and LS241 to several**
956 ***B. lactucae* effectors.** Photos are representative of a typical leaf. *B. lactucae*
957 candidate effectors either elicited necrosis (brown areas) indicative of an immune
958 recognition response (magenta text) or did not elicit a response (aqua text). GFP
959 and HopM1 were used as negative and positive controls for necrosis, respectively.
960 Leaves were collected five days post-infiltration and the first column for each
961 accession shows the uncleared leaf tissue; the second column shows leaf tissue
962 cleared in ethanol.

963

964 **Figure 8. Subcellular localization of three *B. lactucae* WY effectors in lettuce.**

965 Confocal images of lettuce expressing YFP fusion proteins. For YFP-SW4, split
966 images of (A) DAPI, (B) Chloroplast autofluorescence, (C) YFP, and (D) Merged show
967 nuclear localization. For YFP-SW1 (E) and YFP-SW3 (F), merged images of DAPI
968 (blue), chlorophyll autofluorescence (red), and YFP (yellow) show cytoplasmic or
969 periplasmic localization.

970

971

972 **Figure 9. Effect of *B. lactucae* candidate WY effectors on flg22-triggered**

973 **immune response.** Luminescence plots measuring effect of candidate effectors on
974 flg22-triggered PTI induction in *N. benthamiana* leaf discs. (A) Luminescence
975 averaged across biological replicates (14–24 reps each) for each effector over time.
976 (B) Bar plots of the average area under the curve (AUC) for luminescence over 40

977 minutes for each effector (N=14–24), with flg22 (red) or without flg22 (aqua).

978 Asterisks indicate averages in the flg22+ condition that are statistically different

979 from the average of GFP in the flg22+ condition (t-test, $p < 0.05$).

980

981 List of Supplemental Materials:

982 **Supplemental Table 1.** RXLR-like sequences observed within 100 amino acids of
983 the N-terminus of *B. lactuca*e WY proteins, sorted by first amino acid.

984

985 **Supplemental Figure 1.** The number of RXLR-like motifs detected in the first 100
986 amino acids of the N-terminus of *B. lactuca*e WY effectors.

987

988 **Supplemental Figure 2.** Intrinsic disorder of first 150 amino acids of RXLR and WY
989 containing candidate effectors mined from other oomycete genomes.

990

991 **Supplemental Figure 3.** Agroinfiltration results from BLN06-SF5 and sequence
992 comparison between BLN06 between SF5 and BL24.

993

994 **Supplemental File 1.** Sequences and NCBI reference numbers of the 59 WY
995 proteins predicted from the *B. lactuca*e SF5 genome assembly.

996

997 **Supplemental File 2.** Lettuce genotypes tested for recognition of *B. lactuca*e
998 effectors.

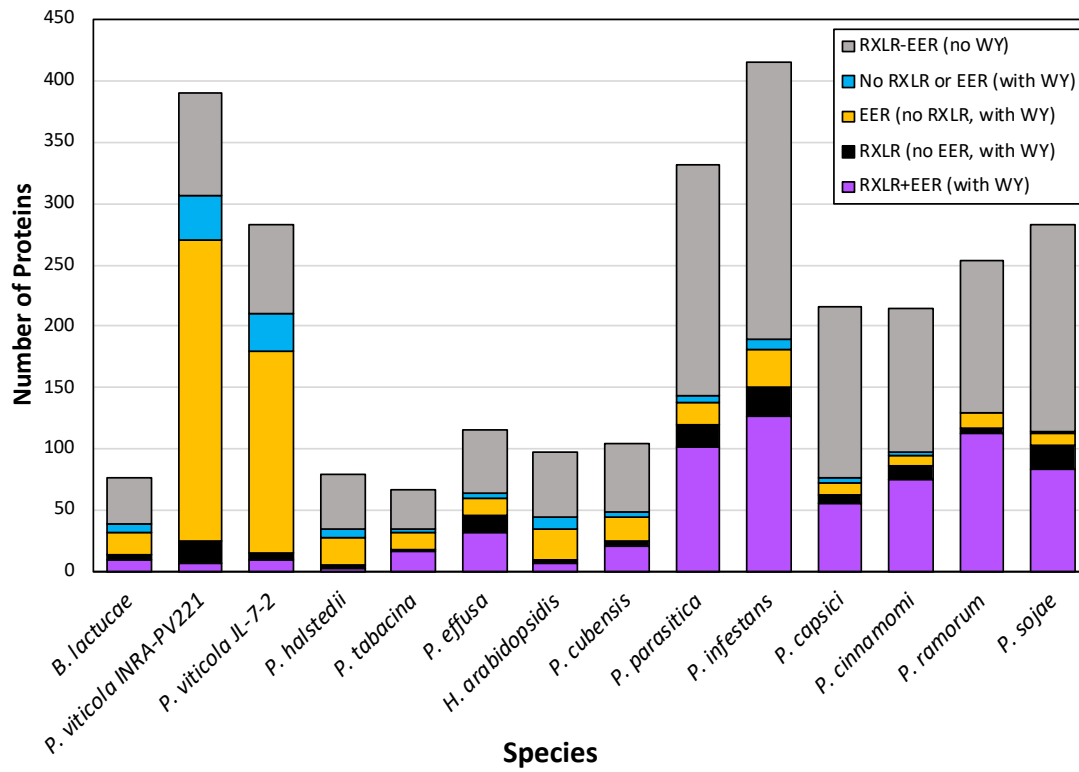
999

1000 **Supplemental File 3.** Primers used in Gateway Cloning of the *B. lactuca*e effectors.

1001

1002

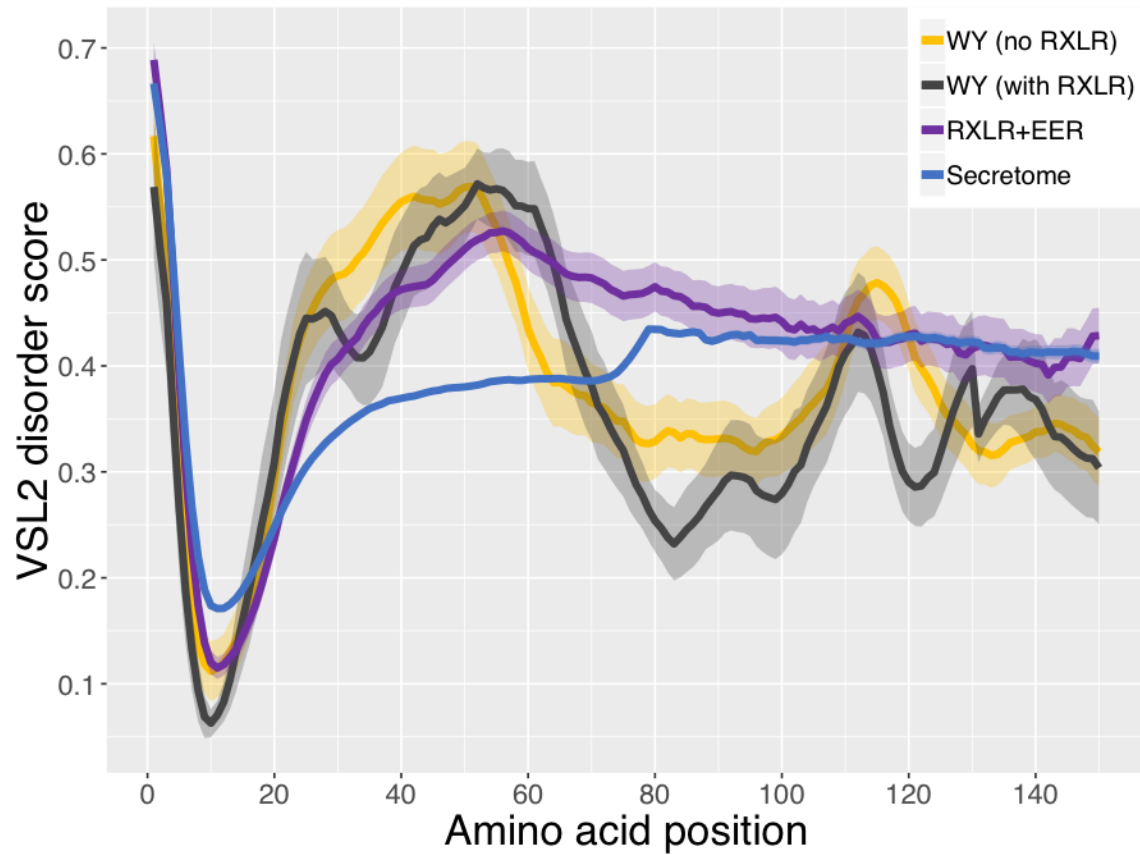
5



6

7 **Figure 2. Distribution of predicted secreted WY effectors with or without RXLR**
8 **and/or EER motifs in the genomes of downy mildew pathogens and**
9 ***Phytophthora* species.**

10



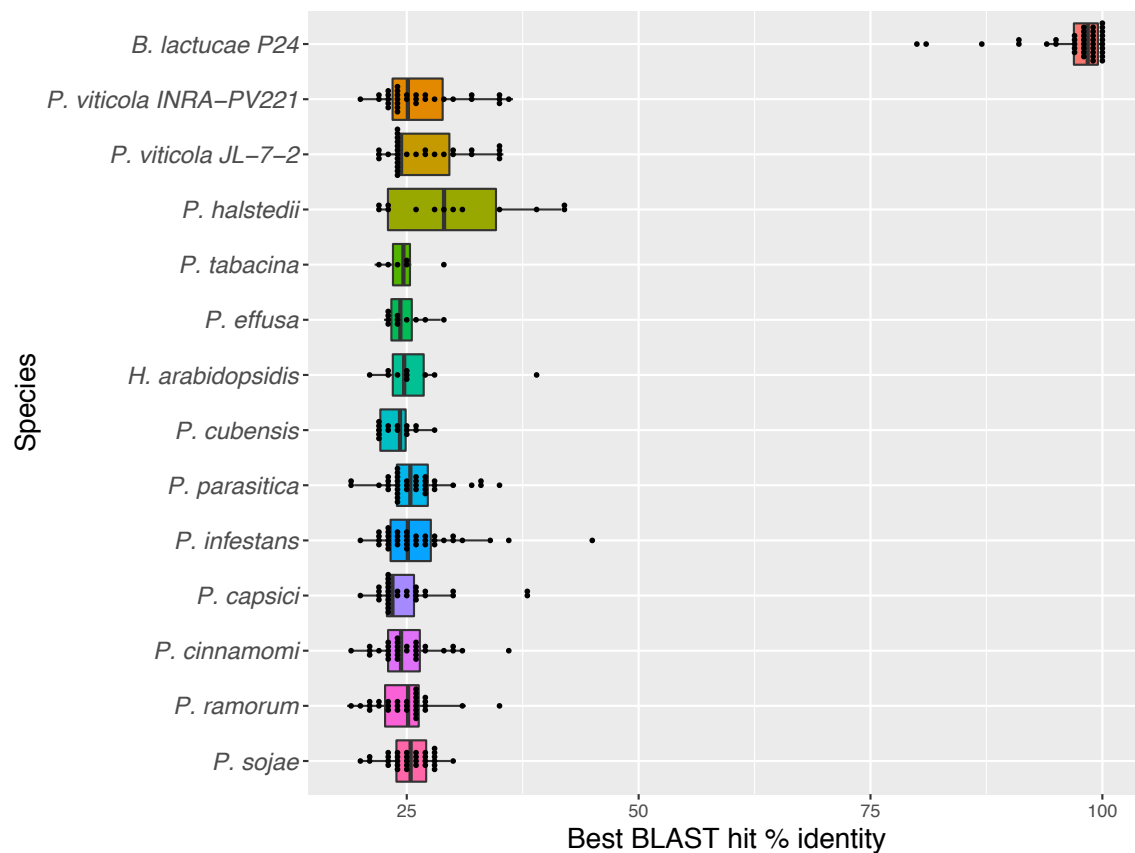
11

12 **Figure 3. Intrinsic disorder in the first 150 N-terminal amino acid sequences**

13 **of RXLR and/or WY containing candidate effectors in *B. lactucae*.**

14

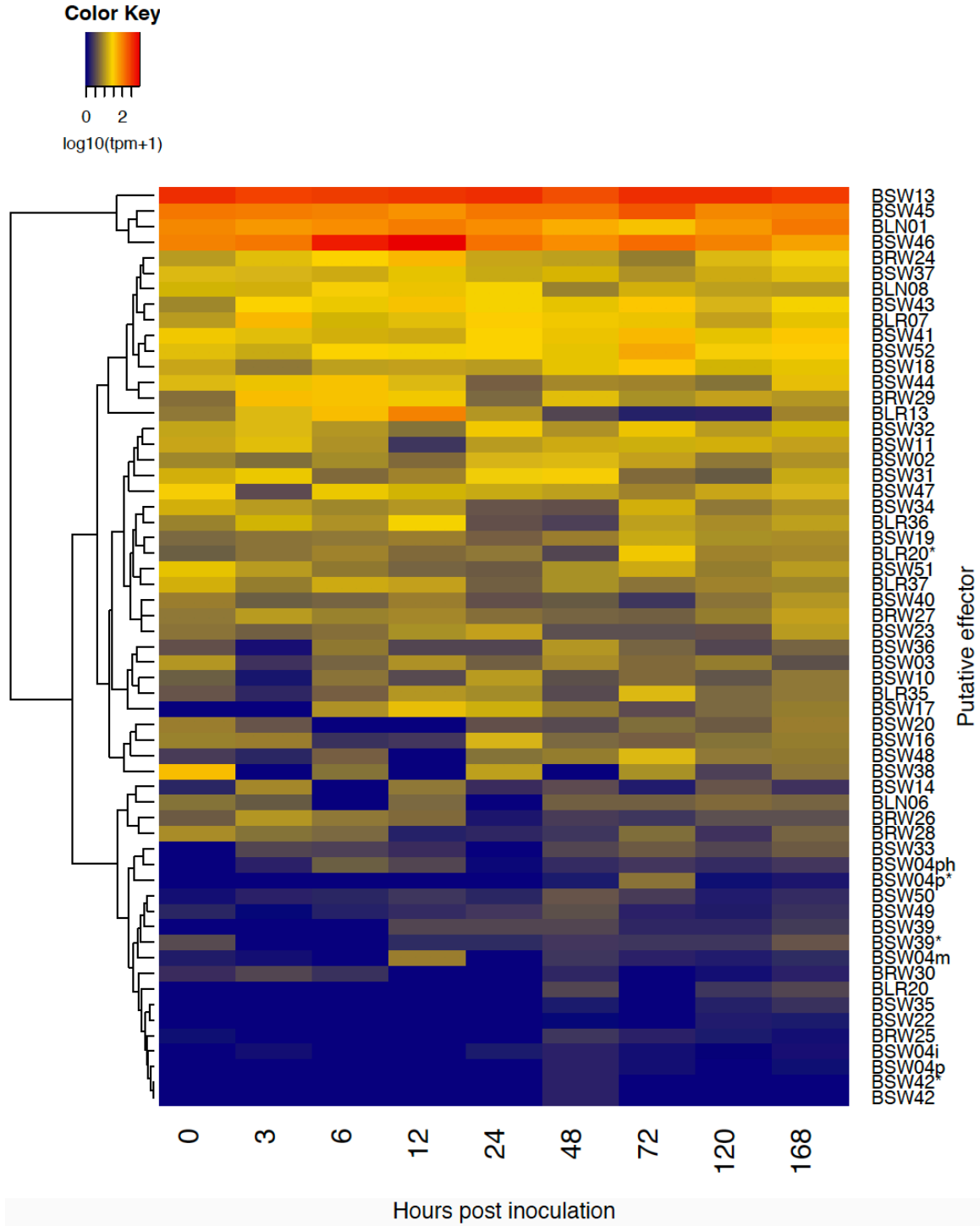
15



16

17 **Figure 4. Lineage specificity of *B. lactucae* candidate secreted WY effectors.**

18



19

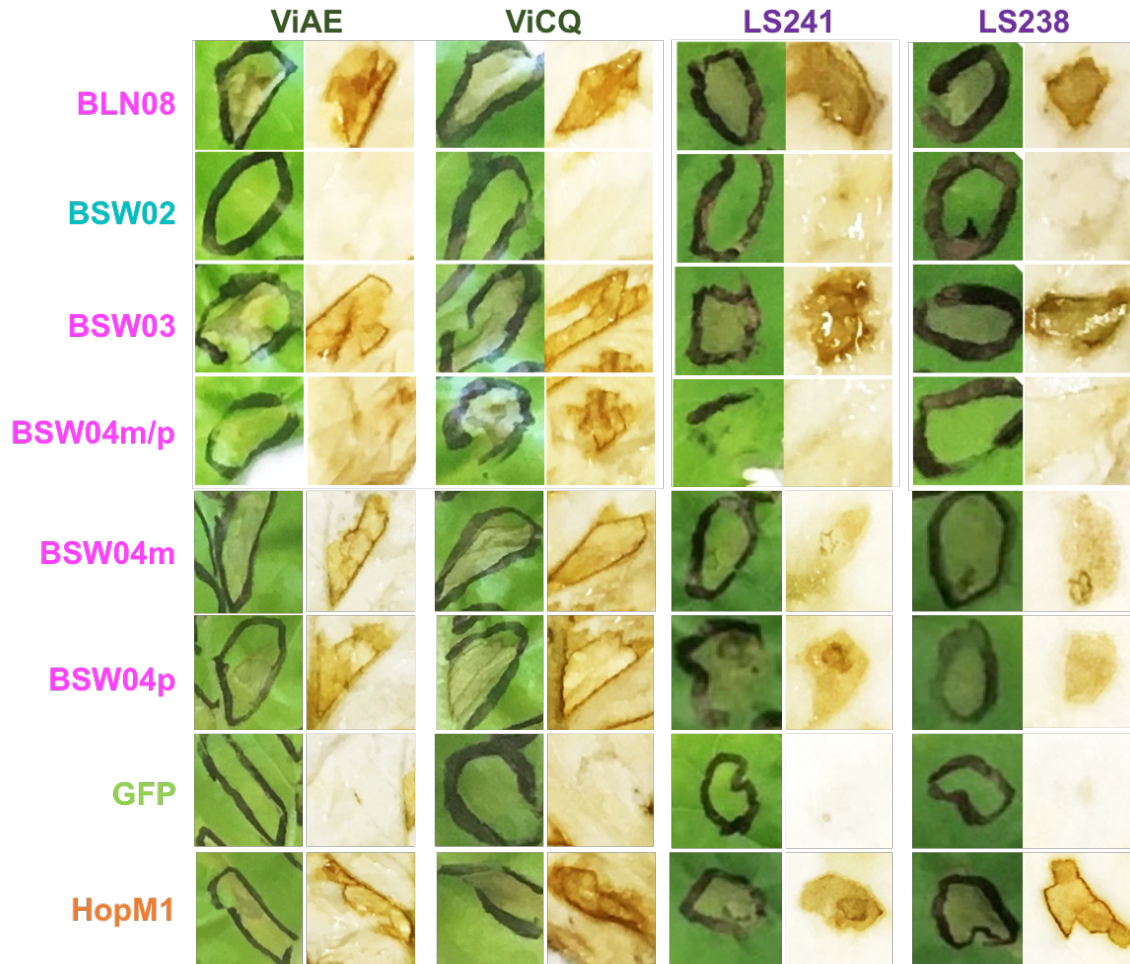
20 **Figure 5. RNA-seq expression levels during infection for the *B. lactucae* WY**
21 **effector candidates.**

Genotype	species	BLR13	BLR36	BLN06	BLN08	BSW03	BSW04m	BSW04m/p	BSW04p	BSW11a	BSW11b	BSW13	BSW14	BSW19	GFP	+control
CGN14312	indica	1.3	3.0	3.3						1.5	1.5	1.5	2.8	1.0	0.8	3.9
CGN14316	indica	0.8	1.5	0.0	0.5	0.4	1.5	2.3	1.0	1.0	1.8	1.6	0.6	0.0	0.4	3.8
CGN5282	saligna	0.0	0.0	0.0	2.5	0.0	0.0	1.5	0.0	0.0	0.0	4.0	4.0	0.0	0.0	4.0
CGN5309	saligna	0.0	2.8	0.0	3.8	0.3	0.6	0.3	1.0	0.0	0.0	4.0	4.0	0.0	0.7	4.0
PI491000	saligna	0.0	0.0	0.0	4.0	0.0	0.0	0.0	0.0	0.3	0.0	1.5	1.6	0.0	0.0	3.9
CGN5329	saligna	0.0	0.0	0.0	2.4	0.1	0.9	1.0	1.8	0.0	0.0	0.0	2.8	2.5	0.3	3.9
CGN5330	saligna	0.0	0.0	0.8	3.3	0.0	0.6	1.0	3.1	0.0	0.0	0.0	3.5	0.0	0.1	4.0
CGN5322	saligna	0.0	0.0	0.0	3.5	0.2	0.1	1.0	2.4	0.0	0.0	0.0	4.0	0.0	0.1	4.0
PI491208	saligna	0.0	0.0	0.0	3.6	0.6	0.6	2.0	3.6	0.0	0.0	0.0	4.0	0.0	0.7	4.0
CGN5318	saligna	0.0	0.0	0.0	3.5	0.8	0.3	2.0	0.3	0.0	0.0	0.0	4.0	0.0	0.1	3.7
PI491207	saligna	0.0	0.0	0.0	4.0	1.1	2.0	2.0	0.5	0.0	0.0	0.0	4.0	0.0	0.2	4.0
25 acc.	saligna	0.0	0.2	0.0	3.0	0.1	0.1	0.3	0.1	0.0	0.0	0.0	3.5	0.1	0.1	3.9
11 acc.	saligna	0.0	2.9	0.0	3.6	0.4	0.3	0.5	0.3	0.0	0.0	0.1	4.0	0.0	0.2	4.0
CGN5309	saligna	0.0	2.5	0.0	3.7	0.3	0.6	0.3	1.0	0.0	0.0	4.0	4.0	0.0	0.3	4.0
CGN5314	saligna	0.0	3.3	0.0	3.8	0.8	0.8	0.8	1.5	0.0	0.0	0.0	4.0	0.0	0.4	4.0
CGN5315	saligna	0.0	1.8	0.0	3.9	0.3	1.0	0.8	1.9	0.0	0.0	0.0	4.0	0.0	0.0	4.0
Blonde	sativa	0.5	0.5	0.0	0.0	0.5	0.5	1.0	0.0	2.0	2.7	0.5	0.0	0.0	0.2	4.0
Capitan	sativa	0.0	0.0	0.0	0.6	0.2	0.2	3.3	3.5	0.0	0.0	0.0	0.0	0.0	0.2	3.8
Capsule	sativa	0.0	0.0	0.0						0.0	0.0	0.0	4.0	0.0	0.0	4.0
Femke	sativa	0.0	0.0	0.0	0.0	0.0	2.4	3.8	3.0	0.0	0.0	0.0	0.0	0.0	0.0	4.0
Fenston	sativa	0.0	0.0	1.0	0.0	0.6	1.3	1.5	2.8	0.0	0.0	0.0	0.0	0.0	0.4	3.6
FrRsal-1	sativa	0.0	1.5	0.0	0.0	0.0	0.1	3.4	0.0	0.0	0.0	0.0	0.0	0.0	0.0	3.8
Ninja	sativa	0.0	1.2	0.0	0.0	0.0	0.2	2.0	3.4	0.0	0.6	0.0	0.0	0.0	0.2	4.0
Pennlake	sativa	0.0	0.0	0.0	0.0	0.0	0.0	2.1	0.0	0.4	0.0	0.0	0.0	0.0	0.0	3.5
PI491226	sativa	0.0	0.0	0.0	3.7	0.6	0.5	1.0	1.5	0.0	0.0	0.0	4.0	0.0	0.1	3.9
RYZ2164	sativa	0.0	0.0	0.0	0.0	0.0	0.0	3.3	0.0	0.0	0.0	0.0	0.0	0.0	0.0	4.0
Salvius	sativa	0.0	0.0	0.0	0.0	0.0	0.0	2.0	0.0	0.0	0.0	0.0	0.0	0.0	0.0	3.6
UCDM14	sativa	0.0	0.0	0.0	0.1	0.1	0.0	0.4	0.0	3.1	0.0	0.0	0.2	0.0	0.4	3.8
Versai	sativa	0.0	0.0	0.4	0.0	0.0	0.7		0.0	3.2	2.3	0.0	0.0	0.0	0.0	4.0
VIAE	sativa	0.0	0.0	0.0	3.4	3.5	3.9	2.0	3.8	0.0	0.0	0.0	2.8	0.0	0.1	3.7
VICQ	sativa	1.0	0.0	0.0	3.9	2.8	3.8	3.3	3.4	0.0	0.0	0.0	3.2	0.0	0.1	3.8
Arm999	serriola	0.0	0.0	0.0	0.0	0.0	3.6	4.0	1.0	0.0	0.0	0.0	0.0	0.0	0.0	4.0
CGN14280	serriola	2.2	0.0	0.5	0.3	0.0	0.0	0.3	0.4	0.0	0.0	0.0	0.0	0.0	0.3	3.3
ISR-380	serriola	0.5	0.5	1.0	0.0	1.0	0.5	0.5	0.5	0.5		0.3	1.0	2.5	0.4	4.0
LS102	serriola	0.0	0.0	0.0	0.0	0.3	0.0	0.0	0.0	0.0	0.0	1.0	2.3	1.3	0.2	4.0
PI491108	serriola	0.0	0.0	0.0	2.1	0.0	0.0	0.0	0.0	0.0	0.0	0.0	3.3	0.0	0.0	4.0
PI491178	serriola	0.0	0.0	0.0		0.0	0.0	0.0	0.0	4.0	0.0	0.0	0.0	0.0	0.0	4.0
CGN14305	virosa	0.0	0.0	0.0	1.5	0.7	0.9	1.5	1.4	0.0	0.0	0.0	2.3	0.0	0.4	3.6
CGN4683	virosa				3.5	0.0	0.0		0.0						0.0	4.0
CGN5333	virosa	0.0	0.0	0.5	0.0	0.1	0.0	0.0	0.0	0.0	0.0	0.0	2.3	1.5	0.0	3.9
CGN9365	virosa	0.0	0.0	0.0	0.2	0.0	0.8	0.0	0.0	0.0	0.0	0.0	3.8	0.0	0.0	4.0
LS238	virosa	0.0	0.0		1.8	2.0	3.9	0.0	3.6	0.0	0.0	0.0	2.0	0.0	0.0	3.4
LS241	virosa	0.0	0.0	0.0	2.5	2.3	3.9	0.0	3.2	0.0	0.0	0.0	3.5	0.0	0.0	3.1

Color Key	Score
No reaction	0
Mild chlorosis	1
Chlorosis	2
Mild Necrosis	3
Necrosis	4
No data	-

22

23 **Figure 6. Results of the screen for recognition of *B. lactucae* WY effector by**
 24 **diverse genotypes of lettuce.**

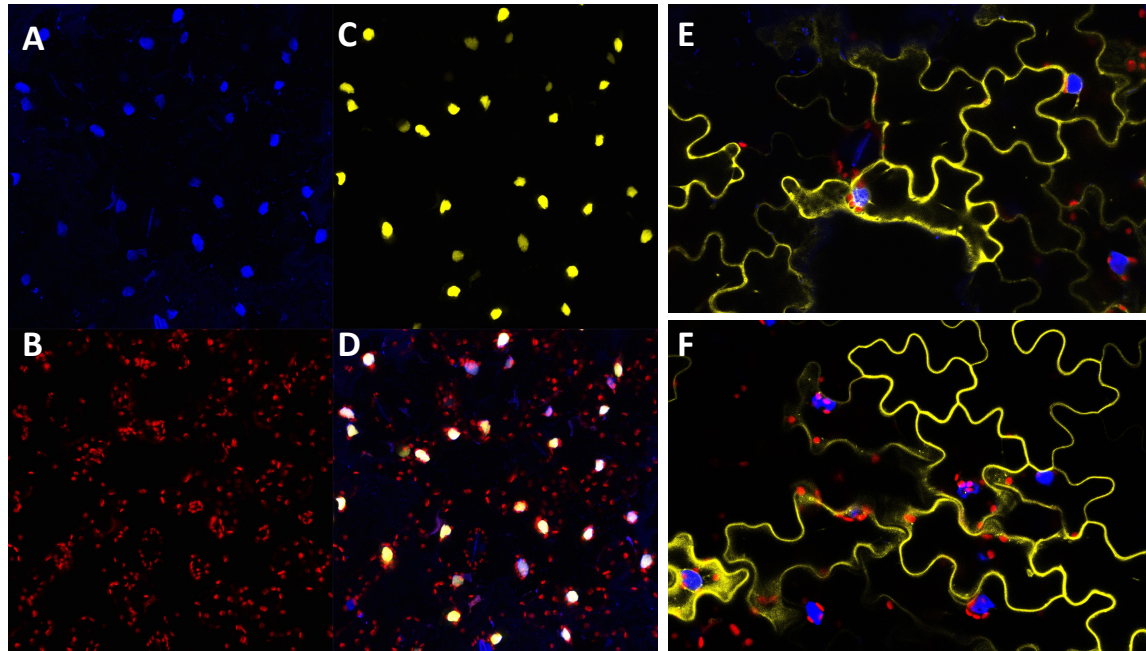


25

26 **Figure 7. Example Agroinfiltration results of reactions of *L. sativa* ViAE and**
27 **ViCQ and their respective progenitor R gene donors *L. virosa* LS241 and LS238**
28 **to several *B. lactucae* effectors.** Photos are representative of a typical leaf. *B.*
29 *lactucae* candidate effectors either elicited necrosis (brown areas) indicative of an
30 immune recognition response (magenta text) or did not elicit a response (aqua
31 text). GFP and HopM1 were used as negative and positive controls for necrosis
32 respectively. Leaves were collected 5 days post infiltration and the first column for
33 each accession shows the uncleared leaf tissue; the second column shows leaf tissue
34 cleared in ethanol.

35

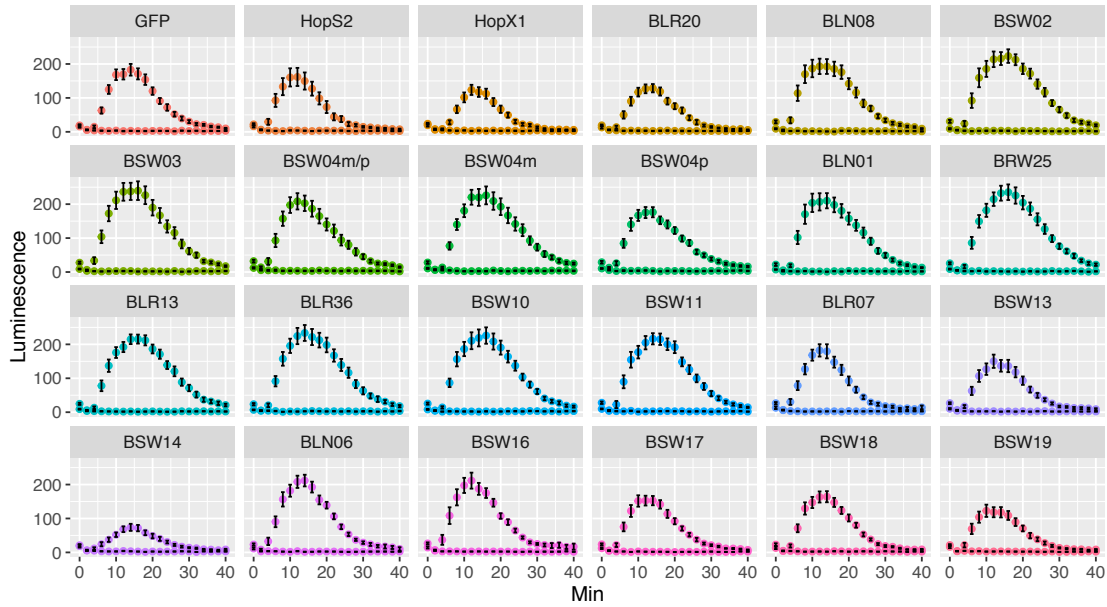
36



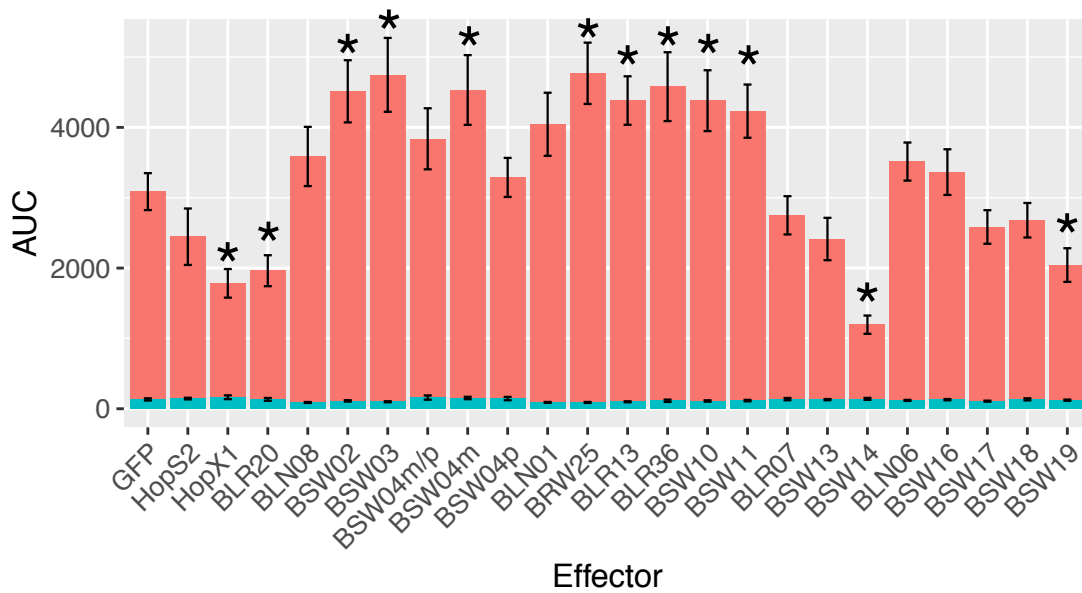
37

38 **Figure 8. Subcellular localization of three *B. lactucae* WY effectors in lettuce.**

39 Confocal images of lettuce expressing YFP fusion proteins. For YFP-SW4, split
40 images of (A) DAPI, (B) Chloroplast autofluorescence, (C) YFP, and (D) Merged show
41 nuclear localization. For YFP-SW1 (E) and YFP-SW3 (F), merged images of DAPI
42 (blue), chlorophyll autofluorescence (red), and YFP (yellow) show cytoplasmic or
43 periplasmic localization.



44



45

46 **Figure 9. Effect of *B. lactucae* candidate WY effectors on flg22-triggered**
47 **immune response.** Luminescence plots measuring effect of candidate effectors on
48 flg22-triggered PTI induction in *N. benthamiana* leaf discs. (A) Luminescence
49 averaged across biological replicates (14-24 reps each) for each effector over time.
50 (B) Bar plots of the average area under the curve (AUC) for luminescence over 40

51 minutes for each effector (N=14-24), with flg22 (red) or without flg22 (aqua) with

52 Asterisks indicate averages in the flg22+ condition that are statistically different

53 from the average of GFP in the flg22+ condition (t-test, $p < 0.05$).

54